Accepted Manuscript

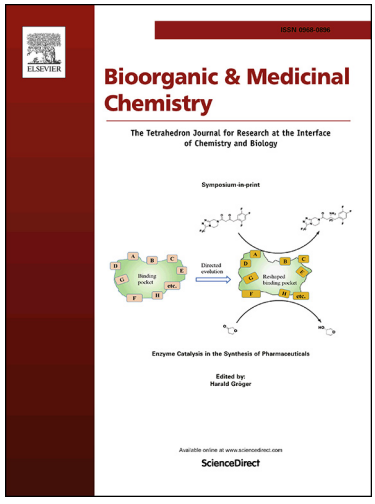

Highly potent and selective aryl-1,2,3-triazolyl benzylpiperidine inhibitors toward butyrylcholinesterase in alzheimer's disease

Peterson de Andrade, Susimaire P. Mantoani, Paulo Sérgio Gonçalves Nunes, Carlos Roca Magadán, Concepción Pérez, Danilo Jordão Xavier, Elza Tiemi Sakamoto Hojo, Nuria E. Campillo, Ana Martínez, Ivone Carvalho

PII: S0968-0896(18)31817-0
DOI: https://doi.org/10.1016/j.bmc.2018.12.030
Reference: BMC 14679

To appear in: *Bioorganic & Medicinal Chemistry*

Received Date: 24 October 2018
Revised Date: 18 December 2018
Accepted Date: 21 December 2018

Please cite this article as: de Andrade, P., Mantoani, S.P., Gonçalves Nunes, P.S., Magadán, C.R., Pérez, C., Xavier, D.J., Hojo, E.T.S., Campillo, N.E., Martínez, A., Carvalho, I., Highly potent and selective aryl-1,2,3-triazolyl benzylpiperidine inhibitors toward butyrylcholinesterase in alzheimer's disease, *Bioorganic & Medicinal Chemistry* (2018), doi: https://doi.org/10.1016/j.bmc.2018.12.030

HIGHLY POTENT AND SELECTIVE ARYL-1,2,3-TRIAZOLYL BENZYLPIPERIDINE INHIBITORS TOWARD BUTYRYLCHOLINESTERASE IN ALZHEIMER'S DISEASE

Peterson de Andrade[1], Susimaire P. Mantoani[1], Paulo Sérgio Gonçalves Nunes[1], Carlos Roca Magadán[2], Concepción Pérez[3], Danilo Jordão Xavier[4], Elza Tiemi Sakamoto Hojo[5], Nuria E. Campillo[2], Ana Martínez[2] and Ivone Carvalho[1]*

[1]School of Pharmaceutical Sciences of Ribeirão Preto, University of São Paulo, Av. Café s/n, 14040-930, Ribeirão Preto, SP, Brazil
[2]Centro de Investigaciones Biologicas (CIB-CSIC), Ramiro de Maeztu 9, Madrid-28040, Spain
[3]Instituto de Química Médica (IQM-CSIC), Juan de la Cierva 3, Madrid-28006, Spain
[4]Department of Genetics, Ribeirão Preto Medical School, University of São Paulo, Av. Bandeirantes 3900, 14049-900, Ribeirão Preto, SP, Brazil
[5]Department of Biology, Faculty of Philosophy, Sciences and Letters at Ribeirão Preto, University of São Paulo, Avenida Bandeirantes 3900, 14040-900, Ribeirão Preto, SP, Brazil

* Corresponding author: phone: +55 16 3315 4709; fax: +55 16 33154879; email: carronal@usp.br

Abstract

Acetylcholinesterase (AChE) is the key enzyme targeted in Alzheimer's disease (AD) therapy, nevertheless butyrylcholinesterase (BuChE) has been drawing attention due to its role in the disease progression. Thus, we aimed to synthesize novel cholinesterases inhibitors considering structural differences in their peripheral site, exploiting a moiety replacement approach based on the potent and selective *h*AChE drug donepezil. Hence, two small series of *N*-benzylpiperidine based compounds have successfully been synthesized as novel potent and selective *h*BuChE inhibitors. The most promising compounds (**9** and **11**) were not cytotoxic and their kinetic study accounted for dual binding site mode of interaction, which is in agreement with further docking and molecular dynamics studies. Therefore, this study demonstrates how our strategy enabled the discovery of novel promising and privileged structures. Remarkably, compound **11** proved to be one of the most potent (0.17 nM) and selective (>58,000-fold) *h*BuChE inhibitor ever reported.

Graphical Abstract

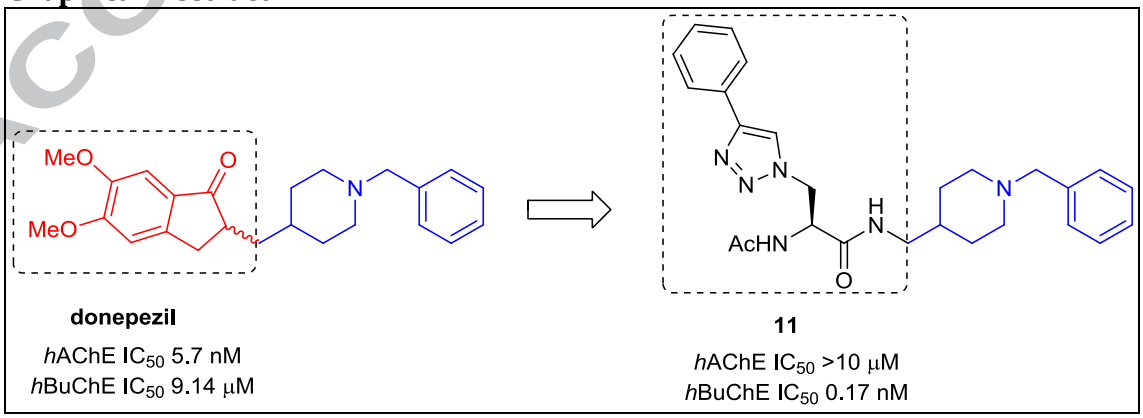

Keywords

Alzheimer's disease, Butyrylcholinesterase, Acetylcholinesterase, Click Chemistry, Inhibitors and Azido amino acids

1. Introduction

Known as the most common type of dementia, Alzheimer's disease (AD) is a severe and progressive neurological disorder characterized by cognitive impairment and irreversible memory loss. Although AD is not fully understood due to its high complexity and its origin is also under scientific debate, the presence of extracellular plaques (accumulation of amyloid-β protein (Aβ)) and neurofibrillary tangles (hyperphosphorylated tau protein) in the brain may possibly have a causal role on the cascade leading to AD. Besides these neuropathological hallmarks, inflammation and oxidative stress processes also contribute to damage of synaptic integrity and neurodegeneration.[1,2] The affected regions by neuronal loss encompass cholinergic neurons, thus compromising learning and memory processes due to deficiency of the neurotransmitter acetylcholine (ACh).[3]

The current treatment is symptomatic and mainly involves restoring of ACh levels through acetylcholinesterase (AChE, EC 3.1.1.7) inhibition by donepezil, rivastigmine and galantamine (cholinesterase inhibitors approved by FDA). AChE is the key enzyme targeted in AD therapy whilst butyrylcholinesterase (BuChE, EC 3.1.1.8), a closely homologous serine hydrolase encoded by different genes and not predominant in the central nervous system (CNS), was previously underestimated.[4-7] However, it has been argued that a switch in focus from AChE to BuChE is owing to a more important role assumed by BuChE in AD advanced stages due to its up-regulation, playing a key function in the disease maintenance and progression.[8,9]

Evidences for BuChE involvement in AD and its role as a considerable drug target have been suggested over the years.[10] In fact, selective BuChE inhibition caused raising of acetylcholine and increased long-term potentiation and learning in rats.[11] Likewise, *in vivo* BuChE inhibition yielded improvement of memory, cognitive functions and learning abilities in cholinergic deficit mice model.[12] Notably, peripheral cholinergic side effects were not observed in these studies. Another expressive result refers to a decreasing of fibrillar Aβ brain plaques (up to 70%) in BuChE knockout mouse, which suggests that the diminished BuChE activity could prove beneficial in AD.[13] Therefore, it seems reasonable to accept that the discovery of highly potent and selective BuChE inhibitors may represent a promising therapeutic approach to AD.[13-15]

Although both enzymes are capable of hydrolyzing ACh, they differ in substrate specificity and sensitivity to inhibitors due to important structural differences in their active site. The catalytic site of both enzymes is located at the bottom of 20 Å deep cavity and the peripheral site is located at the entrance of the cavity. *h*AChE peripheral site is smaller and narrower (about 300 $Å^3$) because it is constituted by aromatic residues whilst in *h*BuChE some of them are replaced by aliphatic residues, consequently yielding a larger region (about 500 $Å^3$) and favouring bulkier ligands binding.[16-18]

In this context, we envisaged the synthesis of novel cholinesterases inhibitors exploiting a relevant method in the discovery of bioactive molecules, such as "click chemistry" (Copper-catalyzed Azide-Alkyne Cycloaddition - CuAAC).[19] Hence, the target compounds **1-12** have been designed based on the potent and selective *h*AChE drug donepezil (Aricept®) keeping the *N*-benzylpiperidine moiety and replacing the 5,6-dimethoxy-1-indanone moiety by other (non)substituted fused (hetero)aromatic scaffolds, tethered to 1,4-disubstituted 1,2,3-triazole ring (series 1), and by azido amino acids to afford 1-substituted-4-phenyl-1,2,3-triazoles (series 2) (Figure 1). Thus, we aimed to evaluate the influence of these replacements upon inhibitory activity and selectivity towards *h*AChE and *h*BuChE considering either a direct coupling (via 1,2,3-triazole ring) or an indirect coupling (via amide bond) to *N*-benzylpiperidine moiety.

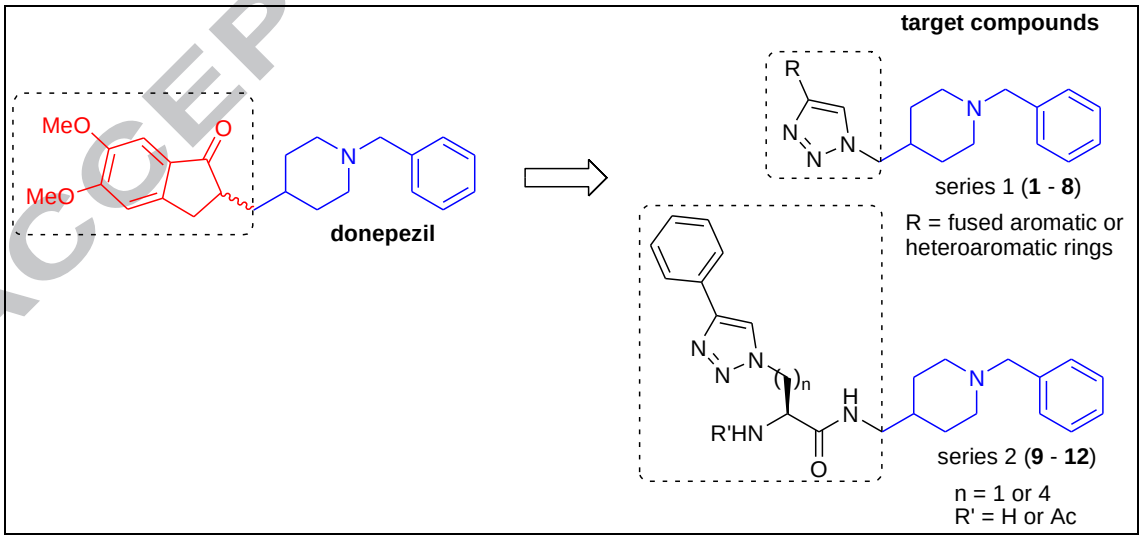

Figure 1. Design of potential cholinesterase inhibitors exploiting a moiety replacement approach considering the potent and selective *h*AChE drug donepezil and a relevant method in drug discovery ("click chemistry").

2. Results and Discussion

2.1 Chemical synthesis

Towards the synthesis of the target compounds **1-8** (series 1), we have proposed a concise route as shown in Scheme 1.

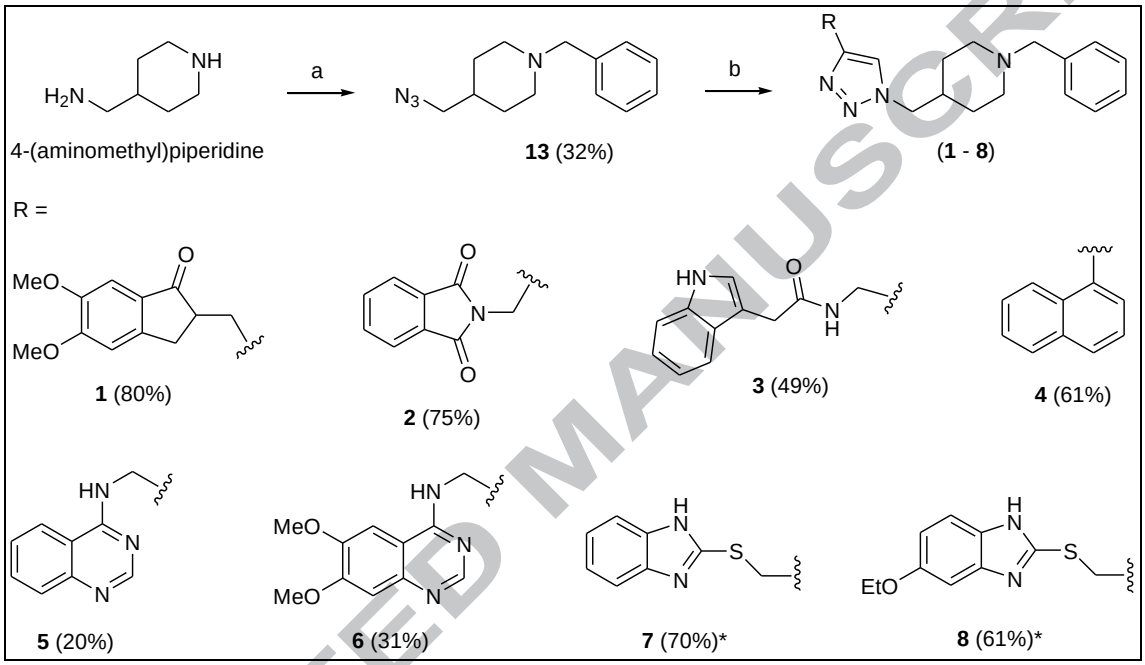

Scheme 1. Synthetic route for the synthesis of the target compounds **1-8** (series 1). Reagents and experimental conditions: a) i. imidazole-1-sulfonyl azide hydrogen sulfate, $CuSO_4$, $NaHCO_3$, $MeOH/H_2O$; ii. BnCl, K_2CO_3, acetone; b) terminal alkyne (RCΞCH), $CuSO_4$, sodium ascorbate, DMF, 100ºC under MW (procedure 1) or terminal alkyne (RCΞCH), $CuSO_4$, sodium ascorbate, $EtOH/H_2O$/1,10-phenanthroline, room temperature (*procedure 2).

The key intermediate **13** was synthesized in two steps (32% overall yield) from readily available 4-(aminomethyl)piperidine by diazo transfer reaction with imidazole-1-sulfonyl azide hydrogen sulfate (synthesized in 50% yield on a gram scale)[20] and $CuSO_4$ in $MeOH/H_2O$ mixture at pH 9 followed by benzylation with BnCl in acetone.[21] Formation of 1,2,3-triazole-1,4-disubstituted ring from **13** and terminal alkynes readily available in our lab [commercial (phthalimide **2a** and naphthyl **4a**) and synthesized (indanone **1a**, indole **3a**, quinazolines **5a**/**6a** and mercaptobenzimidazoles **7a**/**8a** - Supplementary Information)] was initially carried out with $CuSO_4$/sodium ascorbate in DMF under microwave (MW) heating (condition 1)[22] to afford the desired compounds **1-6**, mostly in good yields. Due to degradation problems, an alternative condition

(EtOH/H_2O/1,10-phenanthroline mixture at room temperature)[23] was necessary to obtain compounds **7** and **8** in good yields (70% and 61%, respectively).

Towards the synthesis of the target compounds **9-12** (series 2), two azido amino acid precursors [Fmoc-L-Ala(N_3)-OH (**15**) and Fmoc-L-Lys(N_3)-OH (**17**)] were efficiently synthesized in two steps from commercially available Fmoc-L-Asn-OH and Fmoc-L-Lys(Boc)-OH, respectively (Scheme 2).[24,25]

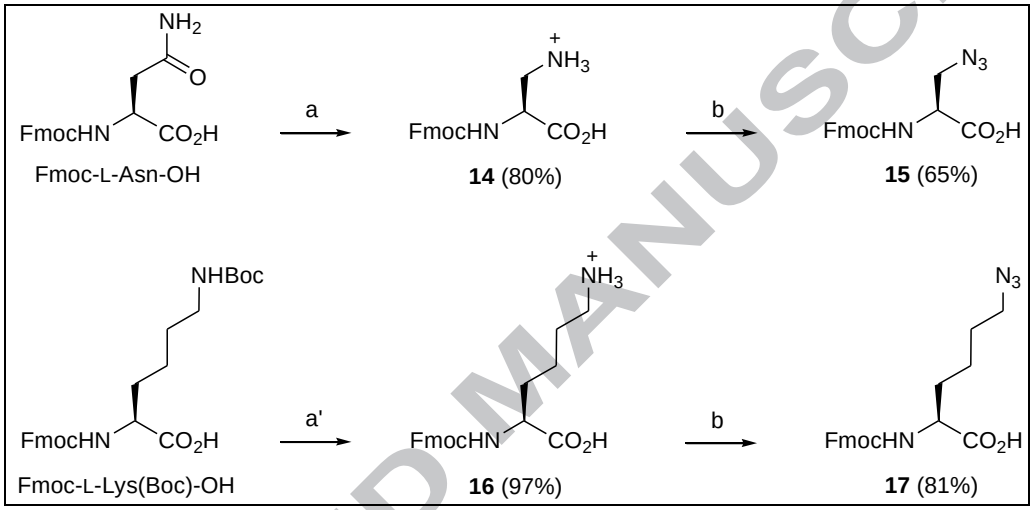

Scheme 2. Synthesis of the azido amino acids **15** and **17**. Reagents and conditions: a) [bis(trifluoroacetoxy)iodo]benzene, pyridine, DMF/H_2O; a') HCl 4.0 M in dioxane; b) imidazole-1-sulfonyl azide hydrogen sulfate, $CuSO_4$, $NaHCO_3$, MeOH/H_2O.

In a Hofmann rearrangement-based procedure, Fmoc-L-Asn-OH was treated with [bis(trifluoroacetoxy)iodo]benzene and pyridine in DMF/H_2O to afford the primary amine **14** (80%), which was converted to the corresponding azido compound **15** (65%) by diazo transfer reaction with imidazole-1-sulfonyl azide hydrogen sulfate and $CuSO_4$ in MeOH/H_2O mixture at pH 9.[24] Likewise, azido compound **17** was also synthesized by the same diazo transfer reaction (81%) from **16**, which was previously obtained by Boc-cleavage (97%) of Fmoc-L-Lys(Boc)-OH in acidic condition.[25] Besides good yields, the syntheses were readily scaled up and pure products were obtained without any further purification for the amide coupling step. Thereafter, we have proposed a straightforward and efficient route for the target compounds **9-12** (series 2) as shown in Scheme 3.

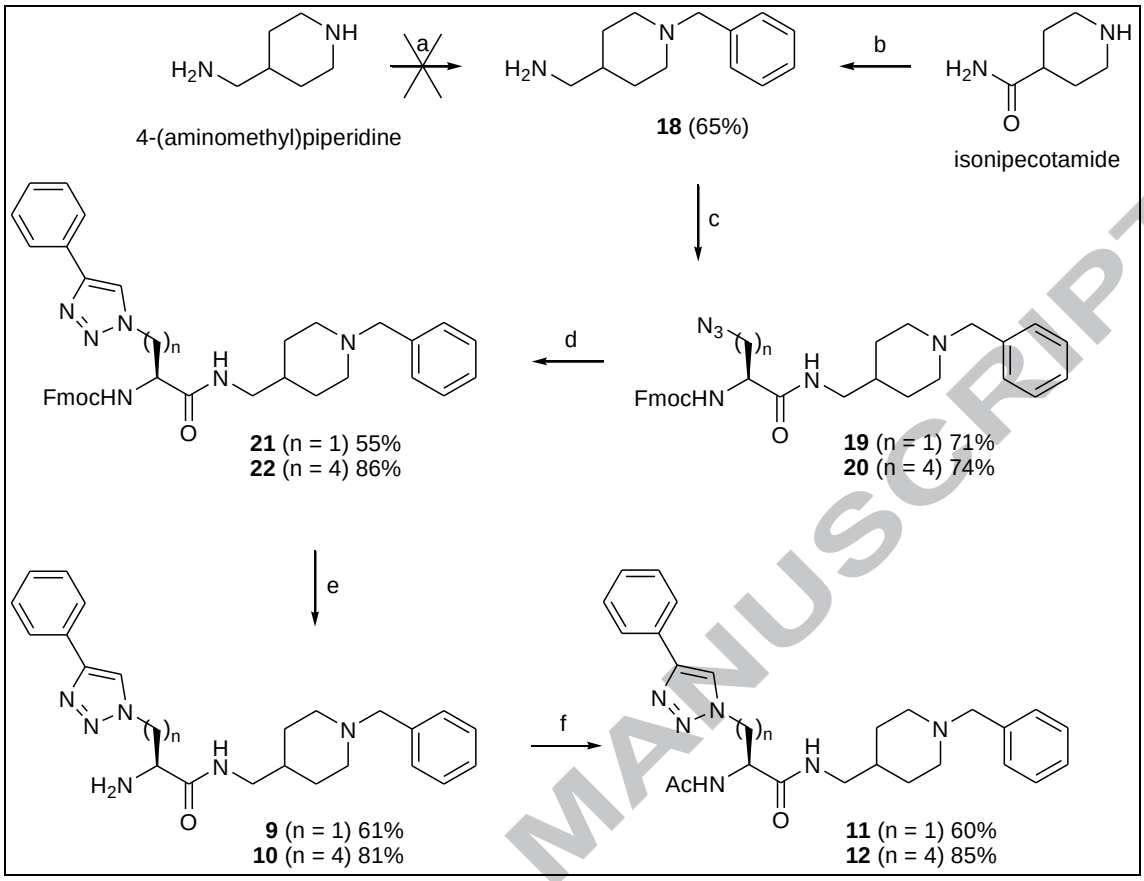

Scheme 3. Synthetic route for the synthesis of the target compounds **9-12** (series 2). Reagents and conditions: a) C_6H_5CHO, $NaBH(OAc)_3$, DCM, $N_{2(g)}$; b) i. BnBr, K_2CO_3, EtOH, 90ºC; ii. $LiAlH_4$, DCM/THF, 70ºC, $N_{2(g)}$; c) azido amino acid **15** or **17**, HBTU, DIPEA, DMF; d) phenylacetylene, $CuSO_4$, sodium ascorbate, *t*-BuOH/H_2O/DCM (1:1:1); e) morpholine/DCM (1:1); f) Ac_2O, pyridine.

After some unsuccessful attempts to synthesize the key intermediate **18** in a more direct and atom-efficient way, just one step from commercial 4-(aminomethyl)piperidine by reductive amination with $NaBH(OAc)_3$ and benzaldehyde in DCM,[26] we have found a two-step method from isonipecotamide more suitable. Hence, commercially available isonipecotamide was benzylated with BnBr and K_2CO_3 in EtOH and the crude product reduced with $LiAlH_4$ in THF/DCM to afford compound **18** in 65% overall yield.[27] Despite the vast number of possibilities for amide bond formation (nature of coupling reagent, reaction conditions, reagent stoichiometry, solvent, etc), the amide coupling between the azido amino acids **15**/**17** and the key intermediate **18** was successfully achieved after some initial failures due to difficulties to find out the most convenient condition. Moreover, some by-products formation made the purification also challenging. Thus, the novel Fmoc-protected azido-building blocks **19** and **20** were

synthesized with HBTU as coupling reagent and DIPEA in DMF at room temperature in good yields (71% and 74%, respectively).[28]

In our initial efforts to perform the next step with compounds **19** and **20** through CuAAC reaction (which also present a wide range of procedures), we have tested the procedure previously described.[22] In this case, the formation of 1,2,3-triazole-1,4-disubstituted ring from commercial phenylacetylene with $CuSO_4$/sodium ascorbate in DMF under MW heating was unsuccessful due to several by-products formation. In order to circumvent this problem, a slightly different protocol in another solvent system (*t*-BuOH/H_2O/DCM 1:1:1) and no heating was tested.[29] Thus, the desired products **21** and **22** were obtained in reasonable yields (55% and 86%, respectively). Further Fmoc-deprotection with morpholine solution in DCM (1:1)[30] afforded the target compounds **9** and **10** in acceptable yields (61% and 81%, respectively), but the classical purification process proved to be difficult because of morpholine contamination and HPLC was needed. In order to investigate whether a small protecting group at the primary amine could play an important role affecting the biological outcome, the corresponding acetylated analogues **11** and **12** were synthesized with Ac_2O and pyridine[31] in reasonable yields (60% and 85%, respectively).

2.2 Cholinesterases inhibition assay

The *in vitro* inhibitory activity of compounds **1-8** (series 1) and **9-12** (series 2) was determined in both cholinesterases by Ellman's assay[32] and it is summarized in Table 1. The whole series 1 proved to be only weak *h*AChE inhibitors (IC_{50} values ranging from >10 μM to 3.94 μM). Similarly, *h*BuChE inhibitory activity was also weak for most compounds (IC_{50} values ranging from >10 μM to 1.91 μM), except **7** (IC_{50} 65 nM). Although some inhibition activity and selectivity have been observed for both enzymes regarding series 1, these results were not so expressive and do not allow a comprehensive study of structure-activity relationships. In general, the low inhibitory activity of this whole series (except compound **7**) suggests a lack of flexibility caused by the direct coupling (via 1,2,3 triazole ring) of benzylpiperidine and the (non)substituted fused (hetero)aromatic moieties. According to our previous work on indolylpiperidines,[15] the capacity of some molecules to change their conformation or shape by folding had a great impact in their binding mode towards *h*BuChE, which

resulted in high inhibitory activity. However, contribution of the non-substituted mercaptobenzimidazole scaffold (**7**) to the potent and selective *h*BuChE inhibition is evident and it indicates that this moiety may have a better fit at *h*BuChE peripheral site compared to *h*AChE. With regard to series 2 (**9**-**12**), none of the target compounds displayed significant inhibitory activity in human recombinant *h*AChE (IC_{50} > 10 μM) compared to donepezil (IC_{50} 5.7 nM). On the other hand, all of them proved to be very active in human recombinant *h*BuChE, being the least active (**12**, IC_{50} 1.02 μM) 9-fold more potent than donepezil (IC_{50} 9.14 μM) and the most active (**11**, IC_{50} 0.17 nM) 53,000-fold more potent. A preliminary analysis suggests that short side chain compounds (**9** and **11**) are much more potent (nM range inhibition) than the long side chain ones (**10** and **12**) (μM range inhibition). Additionally, acetylation of primary amine from **9** (IC_{50} 9.9 nM) to obtain **11** (IC_{50} 0.17 nM) resulted in considerable inhibitory activity improvement (58-fold) that surely makes it one of the most potent and selective (>58,000-fold) *h*BuChE inhibitor ever reported.[10,33]

Table 1. Cholinesterase inhibitory results (*h*AChE and *h*BuChE) based on Ellman modified microplate assay: initial concentration of 10 μM to determine inhibition percentage and subsequent IC_{50} calculation for compounds **1**-**8** and **9**-**12** (donepezil as control).

Structures	Compounds	*h*AChE	*h*BuChE
		IC_{50} ± SEM (μM)	IC_{50} ± SEM (μM)
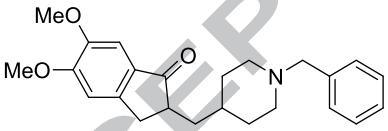	**donepezil**	0.0057±0.0005	9.14±0.56
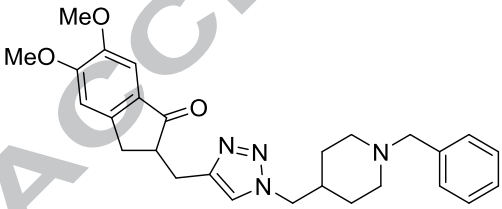	**1**	4.92±0.71	>10
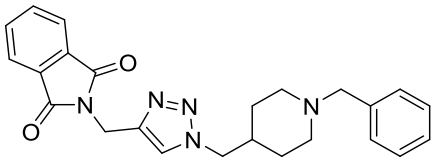	**2**	4.90±0.42	>10
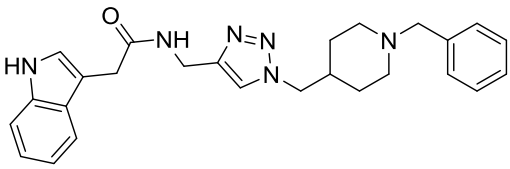	**3**	>10	5.30±0.42

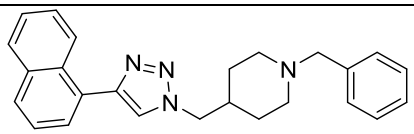	**4**	>10	7.06±0.18
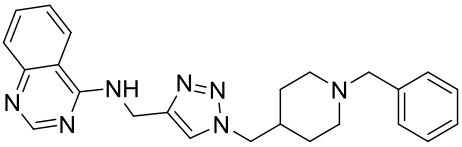	**5**	4.22±0.30	2.95±0.31
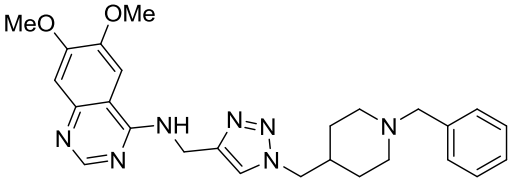	**6**	3.94±0.26	>10
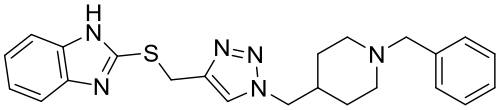	**7**	7.33±0.39	0.065±0.002
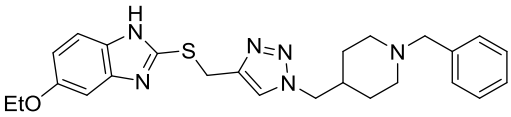	**8**	6.90±0.76	1.91±0.39
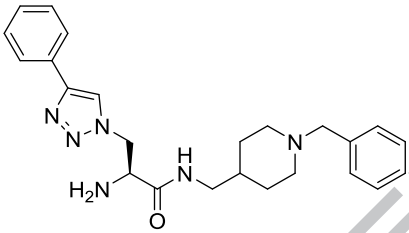	**9**	>10	0.0099±0.0043
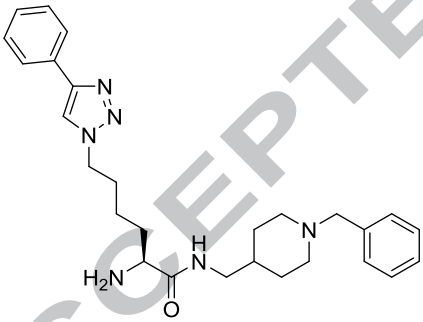	**10**	>10	0.97±0.13
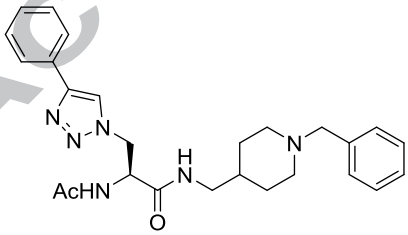	**11**	>10	0.00017±0.000021
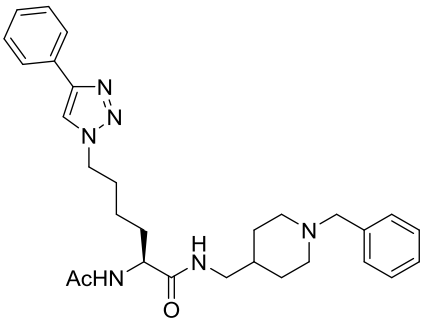	**12**	>10	1.02±0.21

Furthermore, the mechanism of *h*BuChE inhibition for compounds **9** (Figure 2A) and **11** (Figure 2B) was also assessed by means of a kinetic study. This study accounted for mixed-type inhibition models in both cases, which is in accordance with a likely dual binding site (catalytic and peripheral sites) mode of interaction.

A **B**

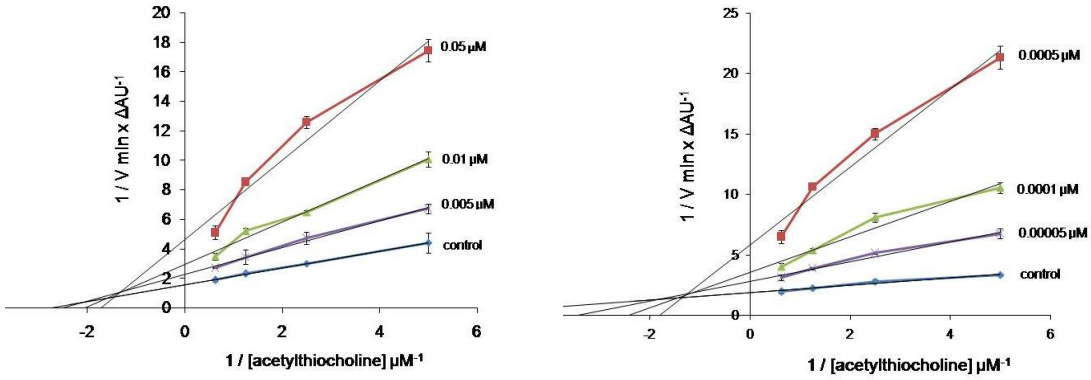

Figure 2. Lineweaver-Burk plots for *h*BuChE inhibition kinetics of compounds **9** (**A**) and **11** (**B**). Reciprocals of enzyme activity *vs* reciprocals of substrate (acetylthiocholine) concentration in the presence of inhibitors at different concentrations.

2.3 Cell viability assays

With the aim to evaluate the cytotoxic effects on human neuroblastoma SH-SY5Y cells line[34] in two recovery periods (24 and 120 hours), the cells were treated with seven concentrations of the series 2 compounds (**9** - **12**) based on their *h*BuChE IC_{50} to obtain a concentration-dependent effect on cell viability. After 24 h recovery, none of them was cytotoxic or significantly inhibited cell growth in the *h*BuChE inhibitory concentration, though compounds **9**, **10** and **12** showed reduction in cell viability at 39.6 nM, 40 µM and 80 µM, respectively (Figure S1). After 120 h recovery, none of them was cytotoxic or significantly inhibited cell growth in the expected concentration, except for the intriguing cell growth inhibition by compound **12** only at 2.5 µM. Interestingly, the cells were able to recover from the mild cytotoxic effect caused by compounds **9**, **10** and **12** after a longer recovery period (Figure S2).

2.4 Docking and molecular dynamic studies

Molecular docking studies[34] were performed for a better understanding of the binding interactions of compounds **9** and **11** in order to rationalize their different potency towards *h*BuChE inhibitory activity. In addition, it was also considered some key information about binding interactions initially provided from a crystal structure (PDB code 4TPK) of *h*BuChE in complex with the potent and selective inhibitor (+)**23** (IC_{50} 13.4 nM).[18] As depicted in Figure 3, the conformational alignment of docked structure **9** (Figure 3A) is very similar to the crystal structure of (+)**23** in *h*BuChE active site (Figure 3B), once the positively charged nitrogen of piperidine also displays a strong cation-π interaction with Tyr332 side chain and an ionic interaction with Asp70 (both from peripheral site). Moreover, 1,2,3-triazole phenyl ring from compound **9** (in optimum distance from the main chain) fully occupies the acyl-binding pocket (Trp231, Leu286, Val288 and Phe329), favouring a π-π aromatic interaction (T-stacking) with Trp231 and Phe329 side chains as well as a π-σ interaction with Leu286 side chain. On the other hand, docked structure **11** displayed different conformation compared to compound **9** and this intriguing result was not initially understood.

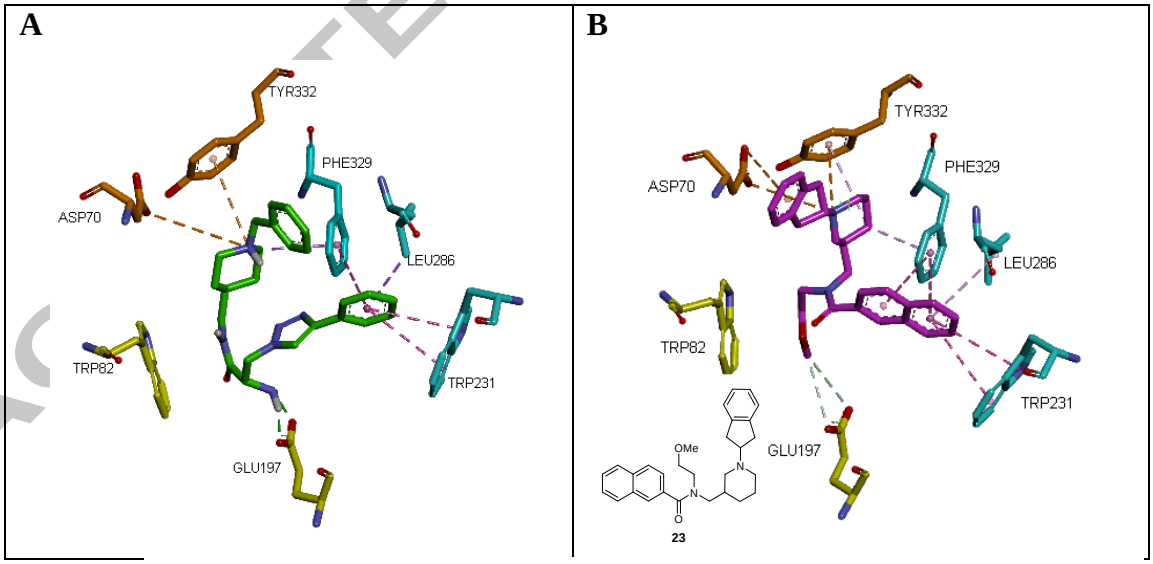

Figure 3. Docking model showing proposed interactions of compound **9** with *h*BuChE (PDB code 1P0I) (**A**) and binding interaction of (+)**23** crystal structure in the active site of *h*BuChE (PDB code 4TPK) (**B**).

Interestingly, a recent crystal structure (PDB code 5DYW) of *h*BuChE in complex with another potent and selective inhibitor (**24**, IC_{50} 4.9 nM)[12] shed light on the outstanding inhibitory activity of compound **11**. As depicted in Figure 4, the conformational

alignment of docked structure **11** (predicted pose) (Figure 4A) is very similar to the crystal structure of **24** in *h*BuChE active site (Figure 4B) and it allows important additional interactions, such as π-π aromatic interaction of the benzyl group with Trp430 and Trp82 side chains (choline-binding pocket) as well as H-bond interaction between the carbonyl group (acetyl) and Thr284 side chain at the entrance of the gorge.

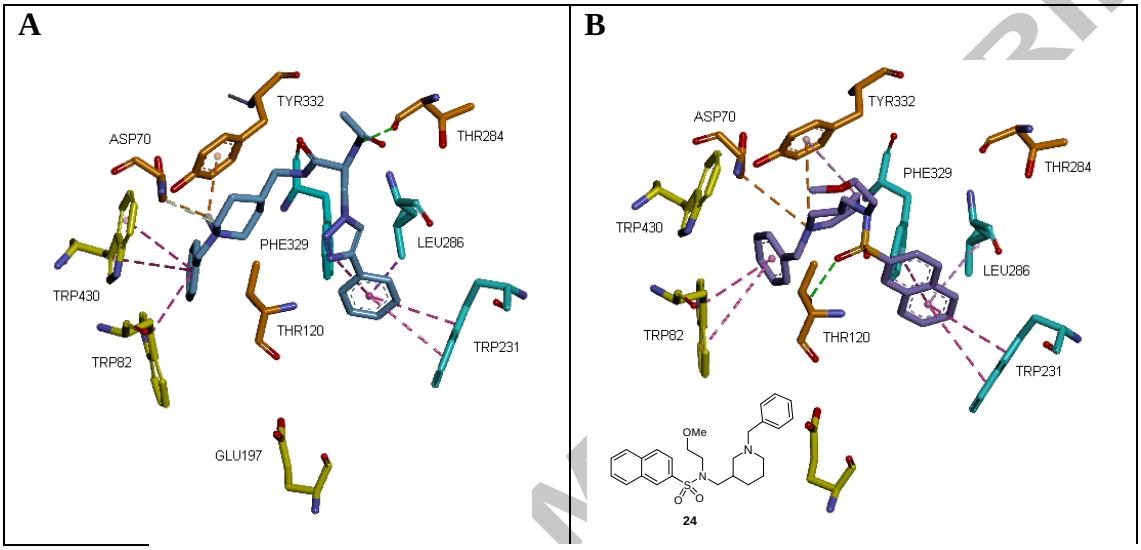

Figure 4. Docking model showing proposed interactions of compound **11** with *h*BuChE (PDB code 1P0I) (**A**) and binding interaction of **24** crystal structure in the active site of *h*BuChE (PDB code 5DYW) (**B**).

Accordingly, the impressive inhibitory activity improvement (58-fold) from compound **9** to **11** may be related to its flipped conformation within the active site (Figure 3A *vs* 4A). It can be inferred that this conformation has been influenced by the acetyl protecting group in compound **11**, which hides the primary amine and abolishes the important interaction with Glu197 observed in compound **9**, allowing an inverted conformation of compound **11** towards the entrance of the gorge, where it is stabilized by H-bond interaction with Thr284 side chain. Indeed, according to the literature Glu197 in *h*BuChE can generate a strong electrostatic potential that draws positively charged ligands into and down the gorge.[18,35,36] In addition, the R-enantiomers of compounds **9** and **11** (not synthesized) were studied *in silico* to show the key role of their chirality. The best docking poses in *h*BuChE for both R-enantiomers showed that the ligands can interact through a π-π aromatic interaction (T-stacking) with Trp231 and Phe329 side chains, in a similar way observed for the S-enantiomers. However, the piperidine ring is reoriented, changing the binding mode in the catalytic gorge and probably their inhibition activity (Figure S3).

Regarding compounds **10** and **12**, although they showed a good fit within *h*BuChE active site and proved to be 9-fold more potent than donepezil, these long side chain compounds are more flexible and may compromise the most favourable conformations toward crucial interactions of 1,2,3-triazole phenyl ring. In this case, even the acetyl group in compound **12** has not affected its biological activity. The docking studies of R-enantiomers of compounds **10** and **12** (not synthesized) showed that the chirality is very important to allow a better binding mode with the target. In both cases, the ligands flexibility is a key property that allows similar poses for S and R, despite the chirality. The best binding pose for compound **10** locates the 1,2,3-triazole phenyl ring in the same place as its S-enantiomer, but the benzylpiperidine group has a different orientation, which does not allow a good fitting in the cavity. On the other hand, compound **12** showed a similar binding mode for S and R enantiomers, but different to the binding pose predicted for compounds **9**, **10** and **11**, since the acyl group does not allow the H-bond interaction with Asp70 (Figure S4).

In general, the low *h*AChE inhibitory activity of compounds **9-12** (IC_{50} > 10 μM) may be explained considering that its acyl-binding pocket is comparatively smaller than *h*BuChE (more details provided in the supporting information). Therefore, the replacement of 5,6-dimethoxy-1-indanone moiety (present in donepezil structure) by amino acids bearing 1,4-disubstituted 1,2,3-triazole phenyl ring abolished the potent inhibitory activity in *h*AChE and drastically enhanced inhibition towards *h*BuChE.

It is also important to highlight that all ligand poses agree to the kinetic studies (mixed-type inhibition model for compounds **9** and **11**), which is in accordance with the dual binding site (catalytic and peripheral sites) mode of interaction showed in the docking studies. Additionally, the previously described docking poses were used as basis for molecular dynamics (MD) simulations[34] of 50 ns length to evaluate the stability of the ligand-protein complexes and how different substituents may affect the binding mode when the ligands converge into a stable pose.

Hence, the root mean square deviation (RMSD) value of *h*BuChE backbone atoms was analysed to estimate the simulation trajectories. By comparing the protein RMSD without ligand (Figure 5A) and the trajectories for compounds **9** (Figure 5B) and **11** (Figure 5C), it was found they are able to stabilize the protein movement turning it into

a more rigid behaviour. As expected, **11** showed higher effect on protein movement stabilization, which is in agreement with the biological result. On the other hand, compounds **10** (Figure 5D) and **12** (Figure 5E) do not affect *h*BuChE behaviour since they shared the same RMSD profile along the simulation.

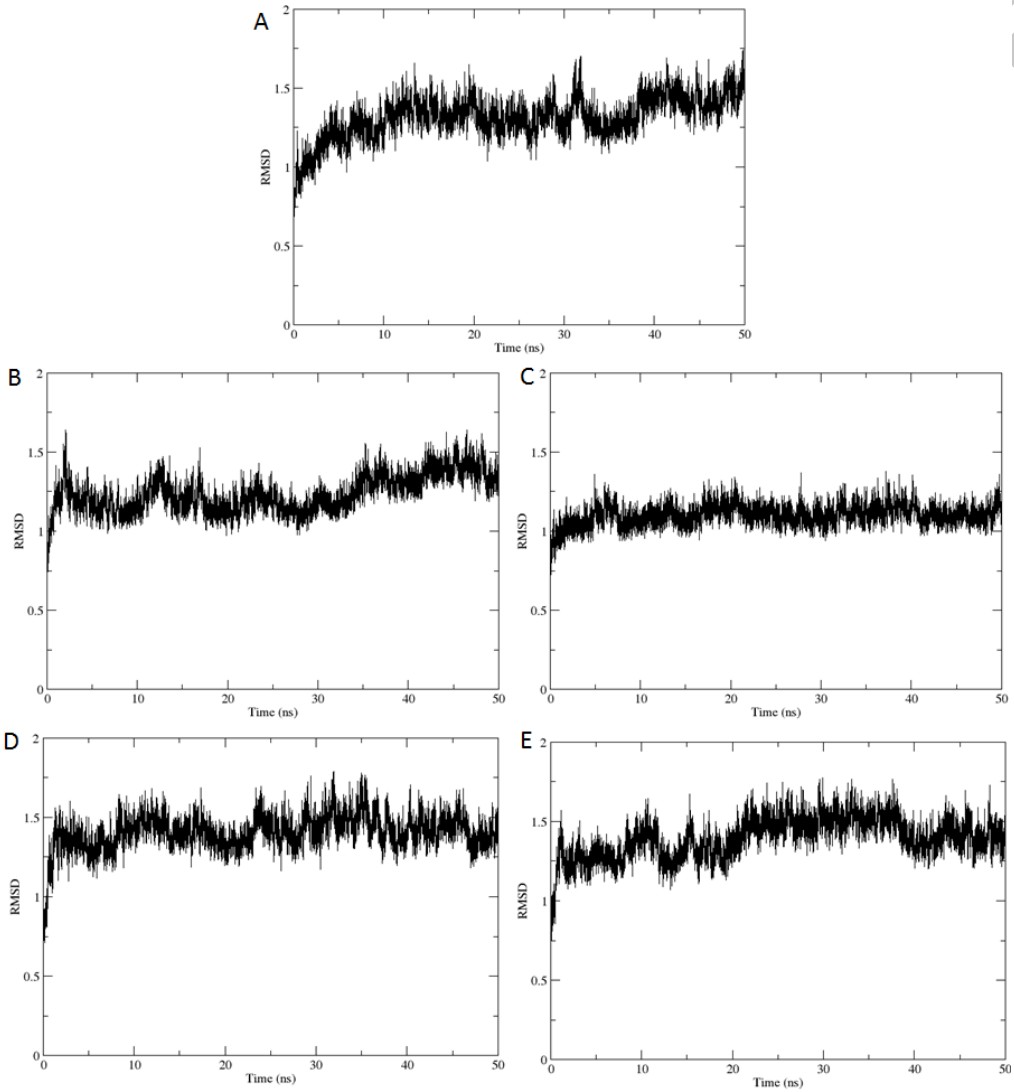

Figure 5. RMSD values for the backbone atoms along 50 ns length MD simulation of *h*BuChE without ligand (**A**), *h*BuChE-compound **9** complex (**B**), *h*BuChE-compound **11** complex (**C**), *h*BuChE-compound **10** complex (**D**) and *h*BuChE-compound **12** complex (**E**).

Based on the MD trajectory, ligands have modified their interactions with the target, converting into a stable pose throughout the simulation. Compound **9** remains stable along the trajectory, maintaining the 1,2,3-triazole ring close to the catalytic residues (Ser198 and His438) and the phenyl ring interacting with the acyl-binding pocket through aromatic interaction (Trp231), but reorienting the benzylpiperidine moiety towards an ionic interaction (Asp70) and changing the primary amine H-bond from

Glu197 to His438 (Figure 6A). On the other hand, compound **11** changes its binding pose along the trajectory due to a steric hindrance that forces different interactions within the active site. In this case, the 1,2,3-triazole and phenyl rings still maintain the same position throughout the trajectory (near to the catalytic residues and the acyl-binding pocket), but the benzylpiperidine moiety is rearranged to a closer interaction with Asp70 and Gln71 by two H-bonds. As a result, the benzyl group orients towards the gorge entrance where its closer interaction with Tyr332 favours the amino acid movement, causing the gorge entrance closing and reducing the access of endogenous substrates (Figure 6B). Regarding compounds **10** and **12**, since they are much more flexible molecules due to their long side chain (4 carbons), they become unable to remain stable in a single pose and fluctuates throughout the simulation.

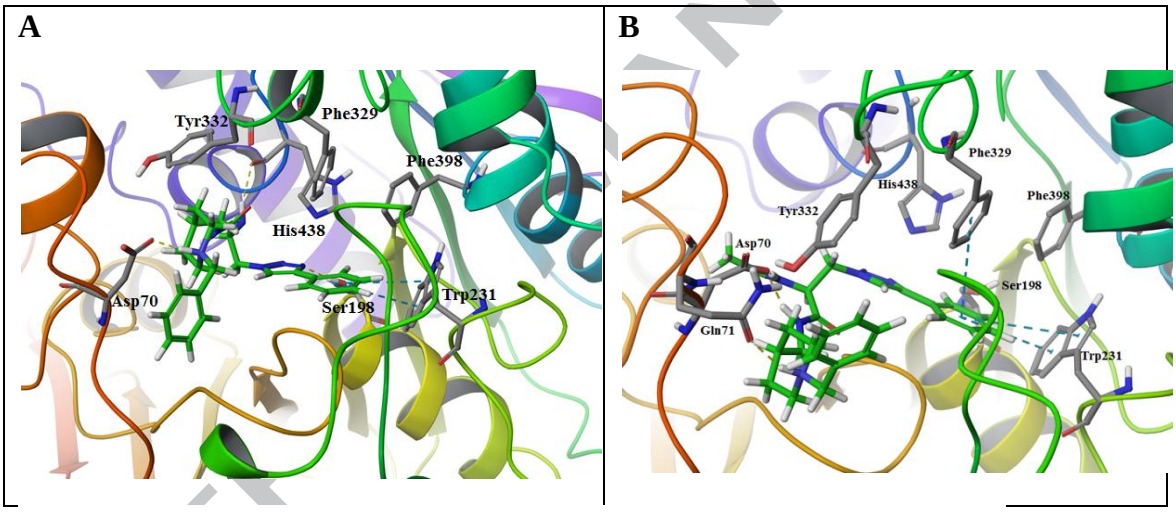

Figure 6. Binding mode of compounds **9** (**A**) and **11** (**B**) with *h*BuChE (PDB code 1P0I) at the final 50 ns of the MD simulation.

As MD simulation results suggested different catalytic gorge behaviour when compounds **9** and **11** interact, a catalytic cavity study variation was carried out as a further investigation to confirm this finding (more details provided in the supporting information). Using the TRAPP software,[37] the last 5 ns of each trajectory were analysed (Figure 7A) observing that the cavity volume decreases due to the movement of both Tyr332 and the acyl-loop when **9** (Figure 7B) and **11** (Figure 7C) interact. Although the cavity volume decreases in both cases, this effect is more significant for *h*BuChE-compound **11** complex, closing the entrance of the gorge. Moreover, it can be observed compound **9** binding mode tends to occupy and open the side-door (specific region/channel in the active site formed by six amino acids), while compound **11**

interacts by moving away from the side-door and keeping those residues in a more rigid way.

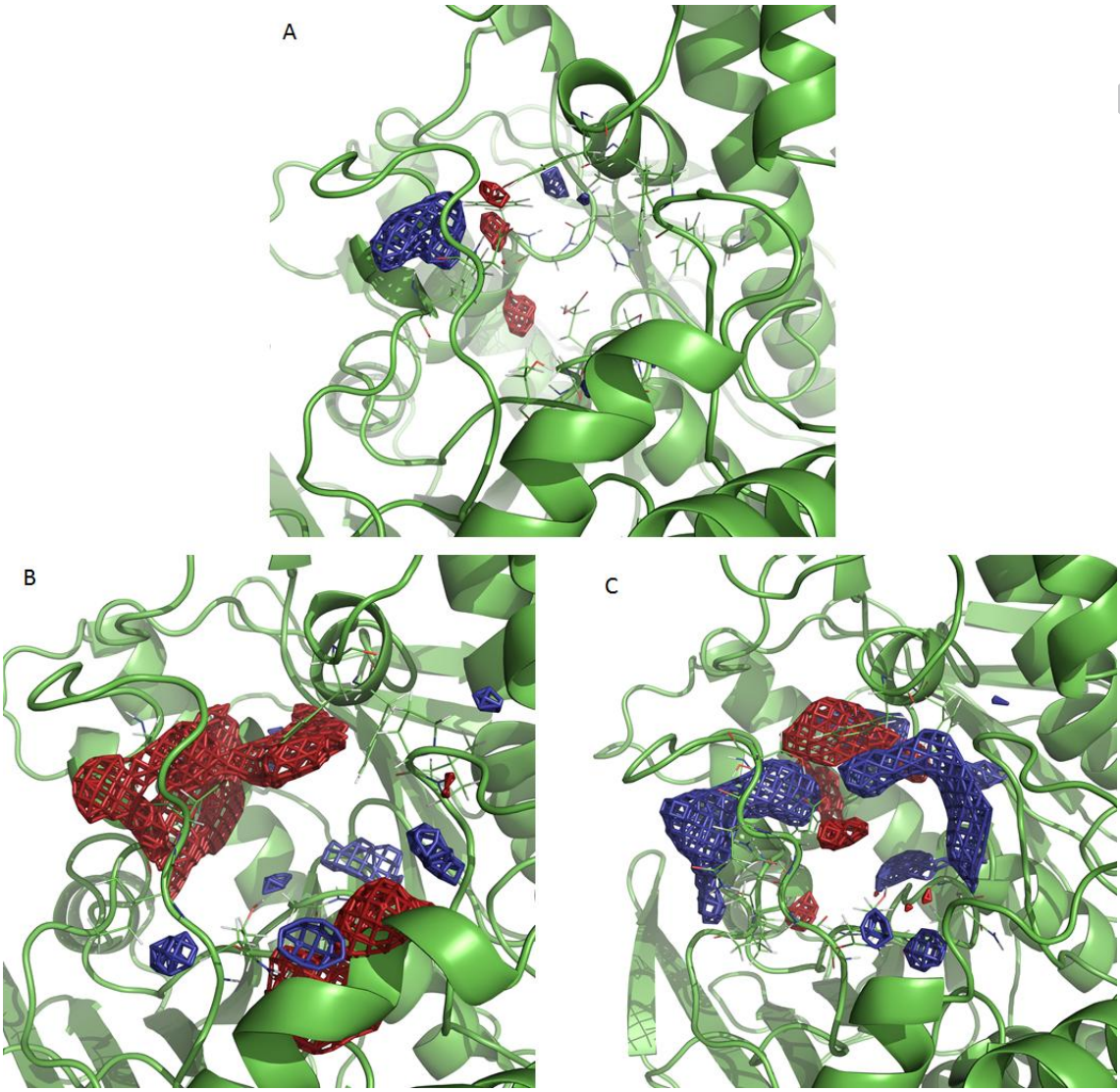

Figure 7. TRAPP results of the catalytic cavity analysis in *h*BuChE (**A**), *h*BuChE-compound **9** complex (**B**) and *h*BuChE-compound **11** complex (**C**). The regions that disappear from the gorge along the simulation are shown in blue and the regions that appear are shown in red. It can be seen that the acyl-loop is moving inwards the cavity in *h*BuChE-compound **11** complex (**C**) and the movement of Tyr332 resulted in the appearance of a new region at the top of the gorge.

2.5 In silico prediction of pharmacokinetic properties

In the context of designing molecules to target the CNS, some physicochemical properties such as molecular lipophilicity (LogP), number of hydrogen bond donors and acceptors (HBD and HBA), molecular weight (MW) and polar surface area (PSA) have been considered important for optimal brain exposure and may define the attributes of successful CNS drug candidates.[38] In this sense, we have calculated some

physicochemical properties using QikProp software v. 2.5[39] to evaluate the drug-likeness of compounds **9** and **11** (Supplementary Information - Table S1). Briefly, most of the calculated parameters are within the acceptable range of effective CNS drugs (LogP < 5, HBD < 3, HBA < 7, MW < 450).[40] More importantly, both compounds can be orally active due to non-violation of Lipinski's rule and the predicted human oral absorption is also promising [**9** (65%) and **11** (81%)] compared to donepezil (100%). The lower values may be explained due to their higher polar surface area, which decreases their brain/blood partition coefficient compared to donepezil.

3. Conclusions

Two small series of *N*-benzylpiperidine based compounds have successfully been designed and synthesized. The proposed synthetic routes were suitable and straightforward to obtain the target compounds **1**-**8** (series 1) and **9**-**12** (series 2), as well as their corresponding precursors (Fmoc-protected azido amino acids and some terminal alkynes). Although most assessed compounds from series 1 exhibited low *h*AChE and *h*BuChE inhibitory activity (μM range), compound **7** (IC_{50} 65 nM) was potent and selective to *h*BuChE. Regarding series 2, the short side chain 1,2,3-triazolyl amino acids **9** (9.9 nM) and **11** (0.17 nM) were not cytotoxic and displayed highly potent and selective inhibition towards *h*BuChE. Additionally, their kinetic studies along with docking and MD studies were important to rationalize their biological outcome. Surprisingly, the replacement of 5,6-dimethoxy-1-indanone moiety (present in donepezil structure) by specific scaffolds tethered via indirect coupling (amide bond) to *N*-benzylpiperidine moiety abolished the potent *h*AChE inhibitory activity and drastically enhanced inhibition towards *h*BuChE. Remarkably, compound **11** proved to be one of the most potent (0.17 nM) and selective (>58,000-fold) *h*BuChE inhibitor ever reported. It is important to highlight that the lead compounds **9** and **11** may be very useful as research tools (i.e. pharmacological probes) to better understand the intriguing role of *h*BuChE not only physiologically and in healthy states, but also in the molecular pathology of severe diseases as Alzheimer. As a follow up work, the crystal structure of *h*BuChE in complex with compounds **9** and **11** would evidence the discussed results on molecular docking and MD simulations. Likewise, the extension of series 2 either by using different protecting groups at the primary amine of **9** or different (non)substituted

fused (hetero)aromatic alkynes would provide new insights of inhibitory activity and selectivity towards *h*AChE and *h*BuChE.

4. Experimental section

4.1 Chemistry

Chemicals were commercially obtained as reagent grade and used without any purification. Thin layer chromatography (TLC - precoated silica aluminium plates) was used for reaction monitoring and compounds were visualized by ultraviolet light (UV - 254 nm), ninhydrin staining solution and/or iodine vapour. Reactions performed at room temperature in this work means a range of temperatures from 20 - 30ºC. CEM Discover Microwave System was used to perform reactions under microwave irradiation in sealed tubes. Biotage SP1-B2C flash chromatography system was used for purification using normal phase cartridges (column 12+S: 21 x 55 mm, 10 g silica flash, 15 mL column volume;10-20 mL/min flow rate) and semi-preparative HPLC purification was run on a Shimadzu Prominence using C18 column, eluting with gradient system (0.1% (v/v) TFA in water and 0.1% (v/v) TFA in methanol). The analytical HPLC was run on a Shimadzu® Shimpack CLC-ODS(M) (4.6 mm i.d x 25 cm) - 5.0 µM particle diameter column, eluting with gradient system 10-90% (0.1% (v/v) TFA in water and 0.1% (v/v) TFA in acetonitrile) and flow rate 1.0 mL/min (column temperature: 40ºC and detector: Diode Array Detector). ^{1}H and ^{13}C NMR spectra were recorded on a Bruker Advance spectrometer at 300, 400 or 500 MHz and chemical shifts are expressed in ppm (δ). Some assignments were aided by COSY (Homonuclear Correlation Spectroscopy) and HMQC (Heteronuclear Multiple Quantum Correlation) spectra. High resolution mass spectroscopy (HRMS) was carried out on a Bruker Daltonics MicroOTOF-Q II ESI-Qq-TOF mass spectrometer using electrospray ionization.

*4.1.1 General procedures for CuAAC reaction to obtain compounds **1** to **8***

Procedure 1 (compounds **1**-**6**): Sodium ascorbate (0.015 mmol) and $CuSO_4$ (1 mg; 0.006 mmol) (6 µL of 1.0 M aq. sol.) were added to a solution of azido **13** (35 mg, 0.15 mmol) and terminal alkyne **1a** - **6a** (0.17 mmol) in DMF (1 mL) in a sealed tube. After 15 min at 100ºC (150 W), toluene (2 x 10 mL) was added for solvents removal under

vacuum. EtOAc (10 mL) was added to the crude and washed with H_2O (2 x 10 mL). Subsequently, the organic layer was dried over $MgSO_4$, filtered, concentrated and purified by flash chromatography [column: 12+S; solvent: Hexane/EtOAc; gradient: 80-100% and 100-100% (v:v); flow: 10 mL/min] to afford 1,4-disubstituted 1,2,3-triazole compounds in good yields.

Procedure 2 (compounds **7**-**8**): To a solution of $CuSO_4$ (0.01 mmol), 1,10-phenantroline (0.01 mmol) and sodium ascorbate (0.20 mmol) in EtOH/H_2O (2:1) (3 mL), stirred at room temperature for 5 min, were added azido **13** (51 mg, 0.22 mmol) and terminal alkyne **7a** or **8a** (0.20 mmol). The reaction was stirred overnight at room temperature and after completion the solvents were removed under vacuum. EtOAc (10 mL) was added to the crude and washed with H_2O (2 x 10 mL). The organic layer was dried over $MgSO_4$, filtered, concentrated and purified by flash chromatography [column: 12+S; solvent: DCM/CH_3OH; gradient: 0-10% and 10-10% (v:v); flow: 9 mL/min] to afford 1,4-disubstituted 1,2,3-triazole compounds in good yields.

4.1.1.1 2-((1-((1-benzylpiperidin-4-yl)methyl)-1*H*-1,2,3-triazol-4-yl)methyl)-5,6 dimethoxy-2,3-dihydro-1*H*-inden-1-one (**1**)

Yield: 80% (55 mg; 120 µmol). ^{1}H NMR (300 MHz, $CDCl_3$) δ_H (ppm): 7.37-7.25 (5H, m), 7.23 (1H, s), 7.12 (1H, s), 6.79 (1H, s), 4.11 (2H, dd, *J* 7.2 Hz, *J* 4.4 Hz), 3.91 (3H, s), 3.87 (3H, s), 3.50 (2H, s), 3.32-3.17 (2H, m), 3.15-2.91 (3H, m), 2.86 (2H, dd, *J* 11.5 Hz, *J* 2.8 Hz), 1.98-1.69 (3H, m), 1.47-1.19 (4H, m). ^{13}C NMR (75 MHz, $CDCl_3$) δ_C (ppm): 206.7, 155.9, 149.6, 144.8, 129.5, 129.3, 128.4, 127.3, 122.5, 107.6, 104.3, 77.6, 63.2, 56.3, 55.7, 53.0, 47.4, 37.0, 31.7, 29.6, 26.8. HRMS (ES^+): *m*/*z* $[M+H]^+$ calculated for $C_{27}H_{33}N_4O_3$: 461.2553; found: 461.2548.

4.1.1.2 2-((1-((1-benzylpiperidin-4-yl)methyl)-1*H*-1,2,3-triazol-4-yl)methyl)isoindoline-1,3-dione (**2**)

Yield: 75% (47 mg; 113 µmol). ^{1}H NMR (400 MHz, $CDCl_3$) δ_H (ppm): 7.85 (2H, dd, *J* 5.5 Hz, 3.1 Hz), 7.71 (2H, dd, *J* 5.5 Hz, 3.0 Hz), 7.54 (1H, s), 7.31-7.24 (5H, m), 4.98 (2H, s), 4.17 (2H, d, *J* 7.2 Hz), 3.50 (2H, s), 2.90 (2H, d, *J* 11.6 Hz), 2.01-1.86 (3H, m), 1.55 (2H, d, *J* 12.0 Hz), 1.37 (2H, q, *J* 11.0 Hz, *J* 9.7 Hz). ^{13}C NMR (101 MHz, $CDCl_3$) δ_C (ppm): 167.8, 142.7, 134.2, 132.2, 129.4, 128.4, 127.3, 123.6, 77.5, 77.2, 63.2, 55.9,

53.0, 37.0, 33.2, 29.7. HRMS (ES^+): *m/z* $[M+H]^+$ calculated for $C_{24}H_{26}N_5O_2$: 416.2087; found: 416.2081.

4.1.1.3 N-((1-((1-benzylpiperidin-4-yl)methyl)-1*H*-1,2,3-triazol-4-yl)methyl)-2-(1*H* indol-3-yl)acetamide (**3**)

Yield: 49% (34 mg; 74 µmol). ^{1}H NMR (400 MHz, CD_3OD) δ_H (ppm): 7.50 (2H, d, *J* 6.9 Hz), 7.35-7.27 (6H, m), 7.18 (1H, s), 7.05 (1H, dd, *J* 8.1 Hz, *J* 1.0 Hz), 6.97 (1H, td, *J* 7.5 Hz, *J* 7.1 Hz, *J* 1.0 Hz), 4.66 (1H, s), 4.41 (2H, s), 4.14 (2H, d, *J* 7.1 Hz), 3.68 (2H, s), 3.52 (2H, s), 3.36 (1H, s), 2.87 (2H, d, *J* 11.9 Hz), 2.01-1.89 (2H, m), 1.74 (1H, ddp, *J* 11.3 Hz, *J* 7.3 Hz, *J* 3.2 Hz), 1.51-1.39 (2H, m), 1.27 (2H, td, *J* 12.2 Hz, *J* 3.2 Hz). ^{13}C NMR (75 MHz, CD_3OD) δ_C (ppm): 173.5, 136.7, 129.5, 127.9, 127.1, 127.0, 123.7, 123.1, 121.2, 118.6, 118.0, 111.0, 107.9, 62.7, 54.9, 52.4, 36.5, 34.4, 32.7, 28.6. HRMS (ES^+): *m/z* $[M+H]^+$ calculated for $C_{26}H_{31}N_6O$: 443.2559; found: 443.2554.

4.1.1.4 1-benzyl-4-((4-(naphthalen-1-yl)-1*H*-1,2,3-triazol-1-yl)methyl)piperidine (**4**)

Yield: 61% (35 mg; 92 µmol). ^{1}H NMR (400 MHz, $CDCl_3$) δ_H (ppm): 8.41-8.30 (1H, m), 7.96-7.84 (2H, m), 7.75 (1H, s), 7.71 (1H, dd, *J* 7.1 Hz, *J* 1.2 Hz), 7.56-7.48 (3H, m), 7.38-7.20 (5H, m), 4.33 (2H, d, *J* 7.2 Hz), 3.52 (2H, s), 2.93 (2H, d, *J* 11.8 Hz), 2.07-1.93 (3H, m), 1.66 (2H, d, *J* 12.7 Hz), 1.46 (2H, qd, *J* 12.3 Hz, *J* 3.8 Hz).^{13}C NMR (101 MHz, $CDCl_3$) δ_C (ppm): 146.8, 137.9, 134.0, 131.2, 129.3, 129.0, 128.6, 128.4, 128.2, 127.4, 127.3, 126.7, 126.1, 125.5, 125.4, 123.2, 63.2, 56.0, 53.0, 37.1, 29.8. HRMS (ES^+): *m/z* $[M+H]^+$ calculated for $C_{25}H_{27}N_4$: 383.2236; found: 383.2231.

4.1.1.5 N-((1-((1-benzylpiperidin-4-yl)methyl)-1*H*-1,2,3-triazol-4-yl)methyl)quinazolin-4-amine (**5**)

Yield: 20% (12 mg; 30 µmol). ^{1}H NMR (400 MHz, $CDCl_3$) δ_H (ppm): 8.68 (1H, s), 7.81 (2H, dd, *J* 15.1 Hz, *J* 8.1 Hz), 7.73 (1H, ddd, *J* 8.3 Hz, *J* 7.0 Hz, *J* 1.3 Hz), 7.60 (1H, s), 7.45 (1H, ddd, *J* 8.2 Hz, *J* 7.1 Hz, *J* 1.2 Hz), 7.33-7.21 (5H, m), 6.82 (1H, t, *J* 5.1 Hz), 4.92 (2H, d, *J* 5.4 Hz), 4.21 (2H, d, *J* 7.1 Hz), 3.49 (2H, s), 2.89 (2H, d, *J* 11.7 Hz), 1.94-1.84 (3H, m), 1.57 (2H, d, *J* 12.6 Hz), 1.37 (2H, qd, *J* 12.3 Hz, *J* 3.8 Hz).^{13}C NMR (101 MHz, $CDCl_3$) δ_C (ppm): 159.3, 155.2, 149.5, 144.4, 138.0, 132.9, 129.3, 128.6,

128.4, 127.3, 126.3, 123.0, 121.0, 115.2, 63.3, 56.0, 53.0, 37.1, 36.6, 29.8. HRMS (ES^+): *m/z* $[M+H]^+$ calculated for $C_{24}H_{28}N_7$: 414.2406; found: 414.2401.

4.1.1.6 N-((1-((1-benzylpiperidin-4-yl)methyl)-1*H*-1,2,3-triazol-4-yl)methyl)-6,7 dimethoxyquinazolin-4-amine (**6**)

Yield: 31% (22 mg; 47 µmol). ^{1}H NMR (400 MHz, $CDCl_3$) δ_H (ppm): 8.49 (1H, s), 7.60 (1H, s), 7.26-7.16 (5H, m), 7.13 (1H, s), 7.10 (1H, s), 7.03 (1H, s), 4.83 (2H, d, *J* 5.2 Hz), 4.14 (2H, d, *J* 7.1 Hz), 3.91 (3H, s), 3.78 (3H, s), 3.44 (2H, s), 2.84 (2H, d, *J* 11.7 Hz), 1.88 (2H, dd, *J* 11.7 Hz, *J* 2.2 Hz), 1.86-1.77 (1H, m), 1.49 (2H, d, *J* 11.7 Hz), 1.33 (2H, qd, *J* 12.4, *J* 3.7Hz). ^{13}C NMR (101 MHz, $CDCl_3$) δ_C (ppm): 158.2, 154.6, 153.7, 149.2, 146.3, 145.1, 137.7, 129.4, 128.4, 127.4, 123.4, 109.0, 107.4, 100.3, 63.2, 56.3, 56.0, 52.9, 37.0, 36.3, 29.7. HRMS (ES^+): *m/z* $[M+H]^+$ calculated for $C_{26}H_{32}N_7O_2$: 474.2617; found: 474.2612.

4.1.1.7 2-(((1-((1-benzylpiperidin-4-yl)methyl)-1*H*-1,2,3-triazol-4-yl)methyl)thio)-1*H*-benzo[*d*]imidazole (**7**)

Yield: 70% (59 mg; 140 µmol). ^{1}H NMR (400 MHz, $CDCl_3$) δ_H (ppm): 7.52 (1H, s), 7.47 (1H, s), 7.34-7.23 (6H, m), 7.2-7.15 (2H, m), 4.41 (2H, s), 4.17 (2H, d, *J* 7.1 Hz), 3.49 (2H, s), 2.86 (2H, d, *J* 11.7 Hz), 1.91 (2H, td, *J* 11.8 Hz, *J* 2.3 Hz), 1.87-1.80 (1H, m), 1.48 (2H, d, *J* 12.6 Hz), 1.31 (2H, qd, *J* 13.0 Hz, *J* 12.5 Hz, *J* 4.0 Hz). ^{13}C NMR (101 MHz, $CDCl_3$) δ_C (ppm): 149.6, 145.0, 137.6, 129.4, 128.4, 127.4, 123.0, 122.5, 63.2, 56.0, 52.9, 36.9, 29.5, 27.0. HRMS (ES^+): *m/z* $[M+H]^+$ calculated for $C_{23}H_{27}N_6S$: 419.2018; found: 419.2011.

4.1.1.8 2-(((1-((1-benzylpiperidin-4-yl)methyl)-1*H*-1,2,3-triazol-4-yl)methyl)thio)-5-ethoxy-1*H*-benzo[*d*]imidazole (**8**)

Yield: 61% (55 mg; 122 µmol). ^{1}H NMR (400 MHz, CD_3OD) δ_H (ppm): 7.64 (1H, s), 7.38-7.21 (6H, m), 6.92 (1H, s), 6.77 (1H, dd, *J* 8.8 Hz, *J* 2.4 Hz), 4.45 (2H, s), 4.16 (2H, d, *J* 7.1 Hz), 4.00 (2H, q, *J* 7.0 Hz), 3.52 (2H, s), 2.82 (2H, d, *J* 11.8 Hz), 2.06-1.83 (2H, m), 1.72 (1H, ddt, *J* 11.4 Hz, *J* 7.5 Hz, *J* 4.1 Hz), 1.38 (3H, t, *J* 7.0 Hz), 1.35-1.24 (2H, m), 1.18 (2H, td, *J* 12.1 Hz, *J* 3.2 Hz). ^{13}C NMR (101 MHz, CD_3OD) δ_C (ppm): 157.2, 145.0, 137.6, 130.9, 129.4, 128.7, 125.1, 113.7, 65.1, 63.9, 56.2, 53.8, 37.8, 37.8,

29.7, 28.4, 15.3. HRMS (ES^+): *m/z* $[M+H]^+$ calculated for $C_{25}H_{31}N_6OS$: 463.2280; found: 463.2274.

*4.1.2 General procedure for Fmoc-deprotection to obtain compounds **9** and **10***

Compound **21** or **22** (75 µmol) was dissolved in morpholine/DCM (1:1) (1 mL) and stirred for 2 h at room temperature. After completion, toluene (2 x 10 mL) was added for solvents removal under vacuum. DCM (15 mL) was added to the crude and washed with H_2O (2 x 10 mL). The organic layer was dried over $MgSO_4$, filtered, concentrated and the crude residue was purified by flash chromatography [column: 12+S; solvent: DCM/CH_3OH; gradient: 0-20% and 20-20% (v:v); flow: 12 mL/min], as well as HPLC [column: C18 (Semi-preparative); solvents: H_2O (0.1% TFA) and CH_3OH (0.1% TFA); isocratic method: 50% (v:v); flow 10 mL/min; injection: 200 µL (3 mg)], to afford the desired compounds.

4.1.2.1 (*S*)-2-amino-*N*-((1-benzylpiperidin-4-yl)methyl)-3-(4-phenyl-1*H*-1,2,3-triazol-1-yl)propanamide (**9**)

Yield: 61% (19 mg; 46 µmol). ^{1}H NMR (500 MHz, CD_3OD) δ_H (ppm): 8.39 (1H, s), 7.83 (2H, d, *J* 7.3 Hz), 7.49-7.44 (7H, m), 7.38 (1H, t, *J* 7.3 Hz), 4.96 (2H, m), 4.48 (1H, t, *J* 5.8 Hz), 4.22 (2H, s), 3.37 (2H, m), 3.29-3.28 (1H, m), 2.95 (1H, dd, *J* 7.2 Hz, *J* 13.5 Hz), 2.85 (2H, q, *J* 13.3 Hz), 1.82 (2H, m), 1.71 (1H, br), 1.42-1.32 (2H, m). ^{13}C NMR (126 MHz, CD_3OD) δ_C (ppm): 167.3, 149.3, 132.3, 131.3, 131.2, 130.4, 130.1, 129.7, 126.7, 123.4, 61.9, 54.1, 53.4, 50.8, 45.2, 35.0, 28.2. HRMS (ES^+): *m/z* $[M+H]^+$ calculated for $C_{24}H_{31}N_6O$: 419.2559; found: 419.2561.

4.1.2.2 (*S*)-2-amino-*N*-((1-benzylpiperidin-4-yl)methyl)-6-(4-phenyl-1*H*-1,2,3-triazol-1-yl)hexanamide (**10**)

Yield: 81% (28 mg; 61 µmol). ^{1}H NMR (500 MHz, CD_3OD) δ_H (ppm): 8.34 (1H, s), 7.82 (2H, d, *J* 7.4 Hz), 7.49-7.44 (7H, m), 7.36 (1H, t, *J* 7.4 Hz), 4.50 (2H, t, *J* 6.6 Hz), 4.24 (2H, s), 3.81 (1H, t, *J* 6.6 Hz), 3.48-3.46 (2H, m), 3.17 (1H, dd, *J* 6.5 Hz, *J* 13.6 Hz), 3.05 (1H, dd, *J* 6.9 Hz, *J* 13.6 Hz), 2.93 (2H, q, *J* 12.7 Hz), 2.05-1.98 (2H, m), 1.92-1.85 (4H, m), 1.79-1.71 (1H, m), 1.46-1.35 (4H, m). ^{13}C NMR (126 MHz, CD_3OD) δ_C (ppm): 170.2, 149.0, 132.3, 131.8, 131.3, 130.4, 130.3, 130.1, 129.5, 126.7, 122.4,

61.9, 54.4, 53.4, 50.9, 49.0, 45.0, 35.1, 31.9, 30.6, 28.3, 22.8. HRMS (ES^+): *m/z* $[M+H]^+$ calculated for $C_{27}H_{37}N_6O$: 461.3029; found: 461.3022.

*4.1.3 General procedure for acetylation reaction to obtain compounds **11** and **12***

Ac_2O (400 µL) was added to a solution of compound **21** or **22** (43 µmol) in pyridine (800 µL) and stirred overnight at room temperature. Afterwards, toluene (2 x 10 mL) was added for solvents removal under vacuum and the crude was purified by flash chromatography [column: 12+S; solvent: DCM/CH_3OH; gradient: 0-10% and 10-10% (v:v); flow: 12 mL/min] to afford the desired compounds.

4.1.3.1 (*S*)-2-acetamido-*N*-((1-benzylpiperidin-4-yl)methyl)-3-(4-phenyl-1*H*-1,2,3 triazol-1-yl)propanamide (**11**)

Yield: 60% (12 mg; 26 µmol). ^{1}H NMR (500 MHz, CD_3OD) δ_H (ppm): 8.29 (1H, s), 7.80 (2H, d, *J* 7.1 Hz), 7.45-7.34 (8H, m), 4.81 (1H, dd, *J* 6.6 Hz, *J* 13.8 Hz), 4.73 (1H, dd, *J* 6.8 Hz, *J* 13.8 Hz), 3.98 (2H, s), 3.20-3.12 (3H, m), 2.97 (1H, dd, *J* 7.1 Hz, *J* 13.5 Hz), 2.56 (2H, q, *J* 10.9 Hz), 1.99 (3H, s), 1.70 (2H, t, *J* 15.0 Hz), 1.63-1.55 (1H, m), 1.32-1.27 (3H, m). ^{13}C NMR (126 MHz, CD_3OD) δ_C (ppm): 173.4, 170.8, 148.8, 131.8, 131.6, 130.4, 130.1, 130.0, 129.5, 126.7, 123.2, 62.3, 54.9, 53.4, 51.8, 49.0, 45.1, 35.6, 28.6, 22.5. HRMS (ES^+): m/z $[M+H]^+$ calculated for $C_{26}H_{33}N_6O_2$: 461.2665; found: 461.2654.

4.1.3.2 (*S*)-2-acetamido-*N*-((1-benzylpiperidin-4-yl)methyl)-6-(4-phenyl-1*H*-1,2,3 triazol-1-yl)hexanamide (**12**)

Yield: 85% (18 mg; 36 µmol). ^{1}H NMR (500 MHz, CD_3OD) δ_H (ppm): 8.32 (1H, s), 7.84-7.80 (2H, m), 7.46-7.42 (7H, m), 7.35 (1H, t, *J* 7.4 Hz), 4.47 (2H, t, *J* 6.8 Hz), 4.17 (1H, dd, *J* 6.1 Hz, *J* 8.2 Hz), 4.10 (2H, s), 3.10 (1H, dd, *J* 6.9 Hz, *J* 13.5 Hz), 3.04 (1H, dd, *J* 6.6 Hz, *J* 13.5 Hz), 2.75 (2H, t, *J* 12.5 Hz), 1.98 (2H, q, *J* 7.3 Hz), 1.94 (3H, s), 1.87-1.75 (3H, m), 1.74-1.64 (2H, m), 1.45-1.30 (6H, m). ^{13}C NMR (126 MHz, CD_3OD) δ_C (ppm): 174.6, 173.4, 148.9, 131.9, 131.8, 130.6, 130.1, 130.0, 129.4, 126.7, 122.2, 55.0, 53.4, 51.1, 44.7, 35.6, 32.2, 30.7, 28.5, 23.8, 22.4. HRMS (ES^+): *m/z* $[M+H]^+$ calculated for $C_{29}H_{39}N_6O_2$: 503.3134; found: 503.3129.

*4.1.4 General procedure for amide coupling reaction to obtain compounds **19** and **20***

HBTU (0.25 g; 0.65 mmol) and DIPEA (0.35 mL; 2.0 mmol) were added to a stirring solution of azido-amino acid **15** or **17** (0.65 mmol) in DMF (10 mL). After 5 min, the key intermediate **18** (0.10 g; 0.50 mmol) diluted in DMF (5 mL) was added and the reaction was stirred overnight at room temperature. DCM (30 mL) was added to the reaction and washed with 5% HCl aq. sol. (20 mL), sat. $NaHCO_3$ aq. sol. (10 mL) and brine (10 mL). The organic layer was dried over $MgSO_4$, filtered, concentrated and the crude was purified by flash chromatography [column: 12+S; solvent: DCM/CH_3OH; gradient: 0-3% and 3-3% (v:v); flow: 8 mL/min] to afford the desired compounds.

4.1.4.1 (9*H*-fluoren-9-yl)methyl(*S*)-1-((1-benzylpiperidin-4-yl)methylcarbamoyl)-2-azidoethylcarbamate (**19**)

Yield: 71% (194 mg; 0.36 mmol). ^{1}H NMR (500 MHz, $CDCl_3$) δ_H (ppm): 7.77 (2H, d, *J* 7.6 Hz), 7.57 (2H, d, *J* 7.2 Hz), 7.40 (2H, t, *J* 7.4 Hz), 7.33-7.22 (7H, m), 6.33 (1H, m), 5.66 (1H, d, *J* 6.1 Hz), 4.53-4.40 (2H ,m), 4.29 (1H, s), 4.21 (1H, t, *J* 6.6 Hz), 3.81 (1H, d, *J* 9.4 Hz), 3.52 (1H, br), 3.48 (2H, s), 3.16 (2H, t, *J* 5.9 Hz), 2.87 (2H, d, *J* 11.4 Hz), 1.92 (2H, t, *J* 11.2 Hz), 1.62 (2H, d, *J* 12.3 Hz), 1.49 (1H, s), 1.35-1.20 (2H, m). ^{13}C NMR (126 MHz, $CDCl_3$) δ_C (ppm): 169.0, 143.7, 141.5, 138.3, 129.3, 128.3, 127.3, 127.2, 125.0, 120.2, 109.7, 67.4, 63.4, 54.3, 53.3, 52.3, 47.3, 45.4, 36.0, 29.9. HRMS (ES^+): *m*/*z* $[M+H]^+$ calculated for $C_{31}H_{35}N_6O_3$: 539.2771; found: 539.2766.

4.1.4.2 (9*H*-fluoren-9-yl)methyl(*S*)-1-((1-benzylpiperidin-4-yl)methylcarbamoyl)-5-azidopentylcarbamate (**20**)

Yield: 74% (215 mg; 0.37 mmol). ^{1}H NMR (500 MHz, $CDCl_3$) δ_H (ppm): 7.76 (2H, m), 7.57 (2H, d, *J* 7.3 Hz), 7.40 (2H, t, *J* 7.5 Hz), 7.33-7.21 (7H, m), 6.16-6.05 (1H, m), 5.38 (1H, d, *J* 7.9 Hz), 4.40 (2H, q, *J* 10.5 Hz), 4.20 (1H, t, *J* 6.8 Hz), 4.12-4.06 (1H, m), 3.48 (2H, s), 3.27 (2H, s), 3.14 (2H, s), 2.86 (2H, d, *J* 11.3 Hz), 1.96-1.78 (4H, m), 1.65-1.56 (4H, m), 1.53-1.36 (3H, m), 1.32-1.22 (2H, m). ^{13}C NMR (126 MHz, $CDCl_3$) δ_C (ppm): 171.5, 156.4, 143.8, 141.5, 138.2, 129.4, 128.3, 127.9, 127.3, 127.2, 125.2, 125.1, 120.2, 67.2, 63.4, 55.1, 53.3, 51.3, 47.3, 45.2, 36.0, 32.2, 29.9, 28.6,22.9. HRMS (ES^+): *m*/*z* $[M+H]^+$ calculated for $C_{34}H_{41}N_6O_3$: 581.3240; found: 581.3235.

*4.1.5 General procedure for CuAAC reaction to obtain compounds **21** and **22***

Sodium ascorbate (8.40 mg; 42 µmol) and $CuSO_4$ (1.64 mg; 10.25 µmol) were added to a stirring solution of Fmoc-protected azido-building block **19** or **20** (205 µmol) and phenylacetylene (35 µL; 307 µmol) in DCM/*t*-BuOH/H_2O (1:1:1) (1.5 mL). The reaction was stirred overnight at room temperature and after completion, toluene (2 x 10 mL) was added for solvents removal under vacuum. DCM (15 mL) was added to the crude and washed with H_2O (2 x 10 mL). The organic layer was dried over $MgSO_4$, filtered, concentrated and the crude was purified by flash chromatography [column: 12+S; solvent: DCM/CH_3OH; gradient: 0-3%, 3-3% and 5-5% (v:v); flow: 9 mL/min] to afford the desired compounds.

4.1.5.1 (9*H*-fluoren-9-yl)methyl(*S*)-1-((1-benzylpiperidin-4-yl)methylcarbamoyl)-2-(4-phenyl-1*H*-1,2,3-triazol-1-yl)ethylcarbamate (**21**)

Yield: 55% (72 mg; 112 µmol). ^{1}H NMR (500 MHz, $CDCl_3$) δ_H (ppm): 7.87 (1H, s), 7.79-7.72 (4H, m), 7.56 (2H, d, *J* 6.8 Hz), 7.38 (4H, t, *J* 7.6 Hz), 7.34-7.17 (8H, m), 6.58 (1H, s), 6.28 (1H, s), 4.97 (1H, d, *J* 11.5 Hz), 4.81 (1H, s), 4.65 (1H, d, *J* 12.3 Hz), 4.44 (2H, q, *J* 9.9 Hz), 4.19 (1H, t, *J* 6.7 Hz), 3.31 (2H, s), 3.11 (1H, dd, *J* 12.6 Hz, *J* 6.2 Hz), 2.99-2.91 (1H, m), 2.72-2.60 (2H, m), 1.67 (2H, q, *J* 10.3 Hz), 1.37 (2H, d, *J* 11.2 Hz), 1.25 (1H, s), 1.14-1.04 (2H, m). ^{13}C NMR (126 MHz, $CDCl_3$) δ_C (ppm): 168.4, 147.9, 143.7, 143.6, 141.5, 141.4, 130.2, 129.3, 129.0, 128.6, 128.3, 128.1, 128.0, 127.3, 127.1, 125.8, 125.1, 121.8, 120.3, 120.2, 67.7, 63.3, 53.1, 51.3, 47.2, 45.3, 35.9, 29.8. HRMS (ES^+): *m*/*z* $[M+H]^+$ calculated for $C_{39}H_{41}N_6O_3$: 641.3240; found: 641.3234.

4.1.5.2 (9*H*-fluoren-9-yl)methyl(*S*)-1-((1-benzylpiperidin-4-yl)methylcarbamoyl)-5-(4-phenyl-1*H*-1,2,3-triazol-1-yl)pentylcarbamate (**22**)

Yield: 86% (120 mg; 176 µmol). ^{1}H NMR (500 MHz, $CDCl_3$) δ_H (ppm): 7.81 (2H, d, *J* 7.6 Hz), 7.76-7.71 (3H, m), 7.58-7.51 (2H, m), 7.39 (4H, q, *J* 7.9 Hz), 7.33-7.20 (8H, m), 6.24 (1H, s), 5.51 (1H, d, *J* 7.7 Hz), 4.40-4.32 (4H, m), 4.17 (1H, t, *J* 6.8 Hz), 4.14-4.04 (1H, m), 3.44 (2H, s), 3.10 (2H, q, *J* 6.1 Hz), 2.82 (2H, d, *J* 11.0 Hz), 2.02-1.94 (2H, m), 1.93-1.82 (4H, m), 1.68 (1H, dd, *J* 13.4 Hz, *J* 6.9 Hz), 1.56 (2H, d, *J* 11.9 Hz), 1.45-1.34 (2H, m), 1.23 (2H, q, *J* 10.3 Hz). ^{13}C NMR (126 MHz, $CDCl_3$) δ_C (ppm): 171.4, 148.0, 143.9, 141.5, 138.4, 130.7, 129.3, 129.0, 128.3, 127.9, 127.2, 127.1,

125.9, 125.2, 125.1, 120.2, 119.8, 67.2, 63.4, 53.3, 50.0, 47.3, 45.2, 36.0, 31.9, 30.0, 29.8, 22.5. HRMS (ES^+): *m*/*z* $[M+H]^+$ calculated for $C_{42}H_{47}N_6O_3$: 683.3710; found: 683.3710.

4.2 Biological assays

4.2.1 Cholinesterases inhibition assay

Based on Ellman's method,[32] the experiments were performed in 96 well microplate and the samples were assessed against human recombinant acetylcholinesterase (*h*AChE) and human serum butyrylcholinesterase (*h*BuChE) according to the literature.[15]

4.2.2 Cell viability assays

Cell viability assay was performed with the XTT (Cell Proliferation Kit II - XTT, Roche Molecular Biochemicals) colorimetric method using SH-SY5Y cell line derived from human neuroblastoma according to the literature.[34]

4.3 Molecular modeling

4.3.1 Docking studies and molecular dynamics

Docking studies and molecular dynamics were carried out using the structure of *h*AChE (PDB 4EY7) and *h*BuChE (PDB 1P0I) according to the literature.[34]

Acknowledgments

This work was supported by Fundação de Amparo à Pesquisa do Estado de São Paulo - FAPESP (grant 2012/14114-5, 2013/50788-3, 2014/04868-8), Coordenadoria de Aperfeiçoamento de Pessoal de Nível Superior (CAPES), Conselho Nacional de Desenvolvimento Científico e Tecnológico (CNPq) Consejo Superior de Investigaciones Científicas - CSIC (grant i-Link0801) and MINECO (CTQ2015-66313-R).

References

1. Masters CL, Bateman R, Blennow K, Rowe CC, Sperling RA, Cummings JL. Alzheimer's disease. *Nat Rev Dis Primers*. 2015;1:1–18.

2. Iturria-Medina Y, Sotero RC, Toussaint PJ, Mateos-Pérez JM, Evans AC. Early role of vascular dysregulation on late-onset Alzheimer's disease based on multifactorial data-driven analysis. *Nat Commun.* 2016;7:1−14.

3. Mufson EJ, Counts SE, Perez SE, Ginsberg SD. Cholinergic system during the progression of Alzheimer's disease: therapeutic implications. *Expert Rev Neurother*. 2008;8:1703−1718.

4. Farina R, Pisani L, Catto M, Nicolotti O, Gadaleta D, Denora N, Soto-Otero R, Mendez-Alvarez E, Passos CS., Muncipinto G, Altomare CD, Nurisso A, Carrupt PA, Carotti A. Structure-Based Design and Optimization of Multitarget-Directed 2HChromen-2-one Derivatives as Potent Inhibitors of Monoamine Oxidase B and Cholinesterases. *J Med Chem.* 2015;58:5561−5578.

5. Martínez A, Rubio AL, Muñoz P, Dorronsoro I, Garcia-Palomero E, Del Monte M, Medina M. WO2005/118570 A1. 2005.

6. Darvesh S, Hopkins DA, Geula C. Neurobiology of butyrylcholinesterase. *Nat Rev Neurosci.* 2003;4:131−138.

7. Giacobini E. Selective inhibitors of butyrylcholinesterase - A valid alternative for therapy of Alzheimer's disease? *Drugs Aging*. 2001;18:891−891.

8. Mesulam MM, Guillozet A, Shaw P, Levey A, Duysen EG, Lockridge, O. Acetylcholinesterase knockouts establish central cholinergic pathways and can use butyrylcholinesterase to hydrolyze acetylcholine. *Neuroscience*, 2002;110:627−639.

9. Mushtaq G, Greig NH, Khan JA, Kamal MA. Status of acetylcholinesterase and butyrylcholinesterase in Alzheimer's disease and type 2 diabetes mellitus. *CNS Neurol Disord Drug Targets*. 2014;13:1432−1439.

10. Li Q, Yang H, Chen Y, Sun H. Recent progress in the identification of selective butyrylcholinesterase inhibitors for Alzheimer's disease. *Eur J Med Chem*. 2017;132:294−309.

11. Greig NH, Utsuki T, Ingram DK, Wang Y, Pepeu G, Scali C, Yu QS, Mamczarz J, Holloway HW, Giordano T, Chen D, Furukawa K, Sambamurti K, Brossi A, Lahiri DK. Selective butyrylcholinesterase inhibition elevates brain acetylcholine, augments learning and lowers Alzheimer β-amyloid peptide in rodent. *Proc Natl Acad Sci*. 2005;102:17213−17218.

12. Košak U, Brus B, Knez D, Šink R, Žakelj S, Trontelj J, Pišlar A, Šlenc J, Gobec M, Živin M, Tratnjek L, Perše M, Sałat K, Podkowa A, Filipek B, Nachon F, Brazzolotto X, Więckowska A, Malawska B, Stojan J, Raščan IM, Kos J, Coquelle N, Colletier JP, Gobec S. Development of an *in vivo* active reversible butyrylcholinesterase inhibitor. *Sci Rep.* 2016;6:39495.

13. Reid GA, Darvesh S. Butyrylcholinesterase-knockout reduces brain deposition of fibrillar beta-amyloid in an Alzheimer mouse model. *Neuroscience*. 2015;298:424−435.

14. Darvesh S. Butyrylcholinesterase as a Diagnostic and Therapeutic Target for Alzheimer's Disease. *Curr Alzheimer Res*. 2016;13:1173−1177.

15. Chierrito TPC, Pedersoli-Mantoani S, Roca C, Sebastian-Pérez V, Martínez-Gonzalez L, Pérez DI, Pérez C, Canales A, Canada, FJ, Campillo NE, Carvalho I, Martinez A. Chameleon-like behavior of indolylpiperidines in complex with cholinesterases targets: Potent butyrylcholinesterase inhibitors. *Eur J Med Chem.* 2018;145:431−444.

16. Conejo-García A, Pisani L, Núñez MC, Catto M, Nicolotti O, Leonetti F, Campos JM, Gallo MA, Espinosa A, Carotti A. Homodimeric Bis-Quaternary Heterocyclic Ammonium Salts as Potent Acetyl- and Butyrylcholinesterase Inhibitors: A Systematic Investigation of the Influence of Linker and Cationic Heads over Affinity and Selectivity. *J Med Chem.* 2011;54:2627−2645.

17. Dighe SN, Deora GS, Mora E, Nachon F, Chan S, Parat MO, Brazzolotto X, Ross B.P. Discovery and Structure-Activity Relationships of a Highly Selective Butyrylcholinesterase Inhibitor by Structure-Based Virtual Screening. *J Med Chem.* 2016;59:7683−7689.

18. Brus B, Košak U, Turk S, Pišlar A, Coquelle N, Kos J, Stojan J, Colletier JP, Gobec S. Discovery, Biological Evaluation, and Crystal Structure of a Novel Nanomolar Selective Butyrylcholinesterase Inhibitor. *J Med Chem.* 2014;57:8167−8179.

19. Zhou CH, Wang Y. Recent researches in triazole compounds as medicinal drugs. *Curr Med Chem.* 2012;19:239−280.

20. a) Goddard-Borger ED, Stick RV. An efficient, inexpensive, and shelf-stable diazotransfer reagent: imidazole-1-sulfonyl azide hydrochloride. *Org Lett.* 2007;9:3797−3800. b) Fischer N, Goddard-Borger ED, Greiner R, Klapötke TM, Skelton BW, Stierstorfer J. Sensitivities of some imidazole-1-sulfonyl azide salts. *J Org Chem.* 2012;77:1760−1764.

21. Diouf O, Depreux P, Chavatte P, Poupaert JH. Synthesis and preliminary pharmacological results on new naphthalene derivatives as 5-HT4 receptor ligands. *Eur J Med Chem.* 2000;35:699−706.

22. Carvalho I, Andrade P, Campo VL, Guedes PM, Sesti-Costa R, Silva JS, Schenkman S, Dedola S, Hill L, Rejzek M, Nepogodiev SA, Field RA. 'Click chemistry' synthesis of a library of 1,2,3-triazole-substituted galactose derivatives and their evaluation against *Trypanosoma cruzi* and its cell surface *trans*-sialidase. *Bioorg Med Chem.* 2010;18:2412−2427.

23. Cruz-Gonzalez DY, González-Olvera R, Negrón-Silva GE, Romero-Lomas L, Gutierrez-Carrillo A, Palomar-Pardavé ME, Romero-Romo MA, Santillan R, Uruchurtu J. One-pot three-component synthesis of new mono- and bis-1,2,3-triazole derivatives of 2-benzimidazolethiol with a promising inhibitory activity against acidic corrosion of Steel. *Synthesis*. 2014;46:1217−1223.

24. Lau, YH, Spring, DR. Efficient synthesis of Fmoc-protected azido amino acids. *Synlett*. 2011;13:1917−1919.

25. a) Galibert M, Renaudet O, Dumy P, Boturyn D. Access to biomolecular assemblies through one-pot triple orthogonal chemoselective ligations. *Angew Chem Int Ed*. 2011;50:1901−1904. b) Isaad ALC, Barbetti F, Rovero P, D'Ursi AM, Chelli M, Chorev M, Papini AM. *N*α-Fmoc-protected ω-azido- and ω-alkynyl-L-amino acids as

building blocks for the synthesis of "clickable" peptides. *Eur J Org Chem*. 2008;5308−5314.

26. Mchardy SF, Bohmann JA, Corbett MR. Design, synthesis, and characterization of novel, nonquaternary reactivators of GF-inhibited human acetylcholinesterase. *J Bioorg Med Chem Lett.* 2014;24:1711−1714.

27. Keita M, Vandamme M, Mahé O, Paquin J. Synthesis of isocyanides through dehydration of formamides using XtalFluor-E. *Tetrahedron Lett*. 2015;56:461−464.

28. a) Li WR, Chou HH. A facile synthesis of amides from 9-fluorenylmethyl carbamates and acid derivatives. *Synthesis*. 2000;1:84−90. b) Lau YH, de Andrade P, McKenzie GJ, Venkitaraman AR, Spring DR. Linear aliphatic dialkynes as alternative linkers for double-click stapling of p53-derived peptides. *ChemBioChem*, 2014;15:2680−2683.

29. Miller N, Williams GM, Brimble MA. Synthesis of fish antifreeze neoglycopeptides using microwave-assisted "Click Chemistry". *Org Lett.* 2009;11:2409−2412.

30. Fields GB. Peptide Synthesis Protocols. In: Pennington MW, Dunn BM, eds. *Methods in Molecular Biology*. Totowa, NJ: Human Press Inc; 1994:

31. Nikolovska-Coleska Z, Meagher JL, Jiang S, Kawamoto SA, Gao W, Yi H, Qin D, Roller PP, Stuckey JA, Wang S. Design and characterization of bivalent Smac-based peptides as antagonists of XIAP and development and validation of a fluorescence polarization assay for XIAP containing both BIR2 and BIR3 domains. *Anal Biochem.* 2008;374:87−98.

32. Ellman GL, Courtney KD, Andres VJr, Featherstone M. A new and rapid colorimetric determination of acetylcholinesterase activity. *Biochem Pharmacol.* 1961;7:88−95.

33. Andrisano V, Naldi M, de Simone A, Bartolini M. A patent review of butyrylcholinesterase inhibitors and reactivators 2010-2017. *Expert Opin Ther Pat.* 2018;28:455−465.

34. Chierrito TPC, Pedersoli-Mantoani S, Roca C, Requena C, Sebastian-Pérez V, Castillo WO, Moreira NCS, Pérez C, Sakamoto-Hojo ET, Takahashi CS, Jiménez-

Barbero J, Canada, FJ, Campillo NE, Martinez A, Carvalho I. From dual binding site acetylcholinesterase inhibitors to allosteric modulators: A new avenue for disease-modifying drugs in Alzheimer's disease. *Eur J Med Chem.* 2017;139:773−791.

35. Felder CE, Botti SA, Lifson S, Silman I, Sussma JL. External and internal electrostatic potentials of cholinesterase models. *J Mol Graphics Modell*. 1997;15:318−327.

36. Nolte HJ, Rosenberry TL, Neumann E. Effective charge on acetylcholinesterase active sites determined from the ionic strength dependence of association rate constants with cationic ligands. *Biochemistry (Moscow).* 1980;19:3705−3711.

37. Kokh DB, Richter S, Henrich S, Czodrowski P, Rippmann F, Wade RC. TRAPP: a tool for analysis of transient binding pockets in proteins. *J Chem Inf Model.* 2013;53:1235−1252.

38. Rankovic Z. CNS drug Design: balancing physicochemical properties for optimal brain exposure. *J Med Chem.* 2015;58:2584−2608.

39. Maestro, version 9.3. Schrödinger Inc., Portland, OR, 2012.

40. Pajouhesh H, Lenz GR. Medicinal chemical properties of successful central nervous system drugs. *NeuroRx*. 2005;2:541−556.

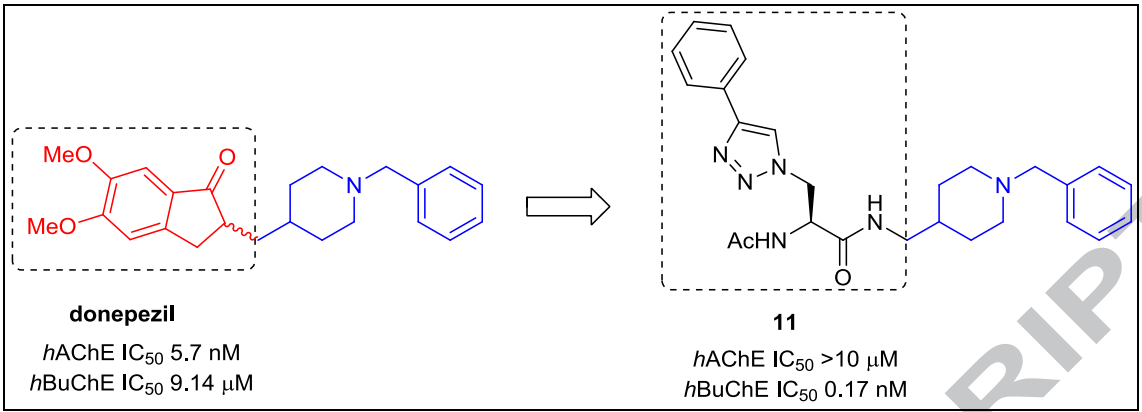

donepezil

*h*AChE IC_{50} 5.7 nM
*h*BuChE IC_{50} 9.14 μM

11

*h*AChE IC_{50} >10 μM
*h*BuChE IC_{50} 0.17 nM

- Highly potent and selective *h*BuChE inhibitors have been successfully synthesized.
- The proposed synthetic approach is efficient and straightforward, which opens up way for the synthesis of chemical libraries.
- The strategy proved to be suitable and enabled the discovery of novel promising and privileged chemical scaffolds.
- The most promising compound is one of the most potent (0.17 nM) and selective (58,000-fold) *h*BuChE inhibitor ever reported.